Review Article

Pulsed field gradients: a new tool for routine NMR

Teodor Parella*

Servei de RMN, Universitat Autònoma de Barcelona, Bellaterra, E-08193 Barcelona, Spain

ABSTRACT: A complete review of 1D and 2D gradient-based NMR experiments published since 1990 is provided. The ease of implementation and the excellent and reproducible results obtained from such experiments offer a powerful tool for the study of molecular structures and dynamics. Thus, when sufficient sample concentration is available, ultra-clean spectra are obtained in very short acquisition times, making the experiments suitable for automated data acquisition. For these reasons, the concept of routine NMR work for chemists has been dramatically changed in the last few years and, with the correct choice of the experiments to be performed, a large number of chemical questions can be resolved in considerably reduced times. However, sensitivity and resolution are dependent on where the PFGs are incorporated into the pulse sequences and, therefore, these two important factors need to be considered in highly demanding applications. Illustrative examples of the most interesting applications to typical organic compounds are given.

KEYWORDS: NMR; pulsed field gradients

INTRODUCTION

The vital importance of NMR in chemistry and biochemistry relies on the evident direct relationship between any given NMR experiment and the molecular information that can be extracted from it. Thus, every experiment is based on some NMR parameter, usually coupling constants or NOE, which is related to a specific molecular parameter (through-bond or through-space connectivities, chemical exchange, molecular motion, etc.). The quantitative measurement of such NMR parameters allows us to obtain valuable information about structural parameters such as dihedral angles, internuclear distances and relaxation and exchange rates. For this reason, the development of new and/or improved NMR methodologies is a key factor to be considered. Nowadays, the enormous suite of NMR experiments available to chemists, many of which use pulsed field gradients (PFGs), find wide application in structural, conformational, stereochemical and dynamic studies on any type of chemical compound. In addition, the successful use of such methodologies in other areas such as molecular diffusion studies,[1–3] solid-state NMR spectroscopy (e.g. high-resolution magic angle spinning)[4] and coupled chromatographic–NMR (e.g. HPLC–NMR) applications[5] also opens up a new future for chemists because of the possibility of analyzing complicated mixtures without the need for chemical separation (e.g. biological fluids, combinatorial chemistry).

Although the idea of using PFGs instead of phase cycling[6,7] for coherence selection in NMR experiments

has been known for some time,[8–10] practical difficulties associated with PFGs, such as eddy currents and B_0 shift effects, prevented their successful application in high-resolution NMR experiments. Since approximately 1991, actively shielded probeheads have been commercially available and, consequently, many gradient-based experiments have recently been proposed which are useful in resolving many chemical questions. The advantages offered by the incorporation of PFGs into high-resolution NMR pulse sequences combined with the advanced software tools available at the present time to acquire and process multi-dimensional NMR experiments has dramatically changed the concept of what is routine NMR for chemists. At present, even a non-experienced user can record and process multi-dimensional NMR experiments automatically simply by the click of a button or by executing a predefined macro.

The main advantages of using PFGs for coherence selection in NMR experiments include (i) a reduction in the number of phase-cycling steps for the suppression of undesired artefacts, (ii) a significant decrease in experiment acquisition times for sufficiently concentrated samples, (iii) the reduction of t_1 noise in two-dimensional spectra, (iv) easier data processing and more accurate spectral analysis, (v) efficient suppression of undesired signals such as the intense solvent signal in H_2O samples or the $^1H–^{12}C$ ($^1H–^{14}N$) magnetization in proton-detected heteronuclear experiments and (vi) a reduction in the dynamic range.

The purpose of this paper is to survey the enormous amount of work, published since 1990, based on the incorporation of PFGs in high-resolution NMR experiments and to illustrate with examples of typical organic compounds the broad spectrum of what are the most interesting current applications found in chemistry. For

* Correspondence to: T. Parella, Servei de RMN, Universitat Autònoma de Barcelona, Bellaterra, E-08193 Barcelona, Spain.
teo@rmn3.uab.es

a more exhaustive description of practical and theoretical properties of PFGs the reader is referred to other excellent reviews.[2,11–19] Experimental details on the practical implementation of some gradient-based experiments have also been published.[20] Finally, PFGs also play an important role in the design of more sophisticated 3D and 4D experiments for studying large [13]C-, [15]N- and/or [2]H-labeled proteins and nucleic acids.[21] Such gradient-based applications have been described during the last 5 years but they are beyond the scope of this review. However, the basic principles describing the function of PFGs in such experiments is a simple extrapolation of the conclusions outlined here.

GENERAL ASPECTS

A PFG is a period during which the B_0 field is made spatially inhomogeneous. Thus, during the application of a PFG, the magnetization is dephased. In general, after applying a PFG of duration τ the spatially dependent phase, $\Phi(r, \tau)$, is given by

$$\Phi(r, \tau) = sB_g(r)\tau \sum_j p_j \gamma_j \qquad (1)$$

where s is a shape factor, $B_g(r)$ is the spatially dependent magnetic field and p and γ are the coherence order and the gyromagnetic ratio, respectively, of the individual j nuclear species involved in the coherence. In their standard configuration, modern spectrometers are usually equipped with a PFG along only the z-axis; in such a case the magnetic field produced by the PFG varies linearly along this axis according to

$$B_g(r) = Gz \qquad (2)$$

where G is the gradient strength expressed in G cm^{-1}. The basis of the gradient-based coherence transfer pathway (CTP) selection procedure is the so-called refocusing condition: *only those CTPs in which the sum of the effects of all applied n PFGs during the sequence is zero just prior to acquisition will be detected*:

$$\sum_{i=1}^{n} s_i G_i \tau_i \left(\sum_j p_{ij} \gamma_{ij} \right) = 0 \qquad (3)$$

In other words, all CTPs having net dephasing at the end of the sequence will not be observed. For simplicity, it can be assumed that all n gradients have the same shape and the same length. Hence Eqn (3) can be simplified to

$$\sum_{i=1}^{n} G_i \left(\sum_j p_{ij} \gamma_{ij} \right) = 0 \qquad (4)$$

This is the most important equation to be considered when selecting the gradient strength ratio in any multidimensional NMR experiment using PFGs.

SENSITIVITY AND RESOLUTION

The sensitivity and resolution of any gradient-based experiment are largely dependent on the position of the PFGs incorporated into it. Basically, PFGs can be used to achieve two different results:

(i) *Selection procedure.* PFGs are applied when the desired magnetization lies in the transverse plane. Only one desired CTP is selected whereas all the others are dephased. This process of selection affords ultra-clean spectra without the need for phase cycling but a sensitivity loss is usually associated with it. The general procedure is as follows: one or several PFGs are included in specific parts of the pulse sequence in order to dephase all transverse coherences. A final PFG, usually applied just prior to acquisition, only rephases the desired CTP. The ratio between all the PFGs must be set according to Eqn (4), so as to ensure refocusing of the desired pathway.

(ii) *Rejection procedure.* In this case, the PFG acts as a purge element which is applied when the desired magnetization is aligned on the z-axis ($p = 0$). All residual transverse coherences are labeled according to their coherence order and are therefore dephased and not detected. This rejection procedure is applied to remove some undesired CTPs. For this reason, a minimal amount of phase cycling is still needed but the subtraction artefacts are largely minimized when compared with an analogous phase-cycled experiment. This approach is not associated with sensitivity losses and is usually applied when the sample concentration is low as, for instance, in studies of large biomolecules. Typical examples would be the purge PFG included during the mixing time in NOESY experiments or in a z-filter and the selection of zz magnetization in HSQC-type experiments.

However, some precautions must be taken into account when designing novel NMR methods aimed at the acquisition of spectra with maximum sensitivity and with signals in the pure absorption lineshape. A PFG inserted into the variable evolution period of a multidimensional experiment selects only one of the two desired CTP (phase-modulated P- or N-type data selection) in each scan:

$$S_P(t_1, t_2) = \exp(i\Omega_1 t_1)\exp(i\Omega_2 t_2) \qquad (5a)$$

$$S_N(t_1, t_2) = \exp(-i\Omega_1 t_1)\exp(i\Omega_2 t_2) \qquad (5b)$$

Therefore, the resulting spectra are usually presented in magnitude mode owing to the undesirable phase-twist lineshape of cross peaks after data transformation. Recording and processing spectra in this way are simple because there is no need to pay attention to the phase errors introduced by the PFGs; such spectra are naturally frequency discriminated in the F_1 dimension.[22,23] This approach is suitable for quick, routine data acquisition in which sensitivity and resolution are not critical.

In order to obtain spectra with absorption mode lineshapes, an alternative has been to modify conventional pulse sequences in order to avoid the application of PFG during the variable evolution period t_1. Although this option generally affords a decrease in the signal intensity by a factor of 2 with respect to the analogous phase-cycled experiment, excellent results are obtained when sensitivity is not the limiting factor. However, an improved approach to obtaining frequency-

discriminated phase-sensitive spectra using the gradient methodology involves recording separate P-type [$S_P(t_1, t_2)$] and N-type [$S_N(t_1, t_2)$] data; this can be done by using the same pulse sequence but inverting the strength of one or more PFGs. The data can then be combined during processing to yield an absorption-mode spectrum.[24] In this so-called echo–antiecho approach, the desired cosine- and sine-modulated data are obtained by combining the P-type and N-type data according to

$$S_{cos}(t_1, t_2) = (S_P + S_N)/2 = \cos(\Omega_1 t_1)\exp(i\Omega_2 t_2) \quad (6a)$$

$$S_{sin}(t_1, t_2) = -i(S_P - S_N)/2 = \sin(\Omega_1 t_1)\exp(i\Omega_2 t_2) \quad (6b)$$

and further processed as complex data by using the States method of frequency discrimination.[25] In this case, there is a sensitivity loss of $2^{1/2}$ compared with the phase-cycled experiment. This data processing is usually available within conventional software packages.

In some experiments, basically those based on the HSQC pulse train, the echo–antiecho approach can be combined with the preservation of equivalent-pathways (PEP) methodology.[26–28] In this case, a sensitivity enhancement of a factor $2^{(n-1)/2}$ can be achieved in an n-dimensional experiment[29–31] when compared with the phase-cycled analog. Thus, in the case of 2D experiments, a theoretical signal-to-noise increase of $2^{1/2}$ for IS systems can be achieved and, therefore, this approach should be used when sensitivity must be maximized. Some examples will be discussed later. Alternatively, pure absorption data could be also obtained by applying the SWAT method,[32] but this approach has not proved popular.

USEFUL GRADIENT BLOCKS

Gradients are usually incorporated into pulse sequences following a series of useful and widely applied building blocks:[11,33]

Phase errors. During the application of a PFG, chemical shift and J-coupling evolutions of the nuclei involved in the selected coherence take place in the usual way. In order to minimize the resulting phase errors due to these evolutions, PFGs are usually included as part of spin echoes, as shown in Fig. 1(a). On the other hand, a PFG can be placed into constant-time defocusing–refocusing periods without further optimizations.

A z-filter. A single PFG inserted into two 90° pulses selects coherence order $p = 0$ during the filter delay whereas transverse magnetization is dephased [Fig. 1(b)]. The mixing time in NOESY experiments is an example of this application.

Refocusing. Two PFGs of equal strength and polarity before and after a 180° pulse applied on a single nucleus provide the opportunity to select terms that have a

transverse spin operator both before and after this pulse [Fig. 1(c)]. In this way, pulse imperfections (transfer from I_z to I_x, or vice versa) are removed and transverse magnetization that does not experience the 180° pulse is dephased. This scheme is also applicable to heteronuclear systems, and is widely used in the INEPT pulse trains which form part of multidimensional HSQC experiments [Fig. 1(d)].

Inversion. If the 180° pulse is used to invert z-magnetization (from z to $-z$), the greatest dephasing of undesired coherences is obtained when the second gradient is applied in the opposite sense to the first [Fig. 1(e)]. In this way, any residual transverse magnetization created by the imperfect 180° pulse is eliminated.

Heteronuclear magnetization transfer. Magnetization transfer between two J-coupled heteronuclei, I and S, is usually achieved by a pair of simultaneous 90° pulses, preceded and followed by delays for J dephasing and rephasing. A simple way to remove unwanted magnetization is to apply a PFG between these two pulses in order to select the desired zz magnetization [Fig. 1(f)]. This building block is largely used in gradient-enhanced multi-dimensional HSQC-type experiments.

Heteronuclear decoupling. In heteronuclear experiments, a single refocusing pulse is often used to remove the effects of the heteronuclear coupling over a period. Thus, if a PFG is applied in the opposite sense (called bipolar gradients), any coherences on I-spin will be rephased whereas the 180° pulse on S acts as a simple inversion pulse [Fig. 1(g)]. The net effect is that the chemical shift of I-spin freely evolves during the overall duration of the two PFGs but the heteronuclear coupling is refocused.

PRACTICAL ASPECTS

Several practical aspects must be taken into account when PFGs are incorporated into any pulse sequence, namely the duration, the shape and the strength of PFG, the use of single z- or multiple-axis PFGs, control of pre-emphasis, the recovery delay needed after applying a PFG, the lock hold device and the gradient amplifier blanking. In practice, most of the described experiments can usually be run on conventional NMR spectrometers equipped with gradients only in the z-axis with a duration of 0.5–2 ms, shaped to sine or Gaussian (1–5% truncated) and with a 100 µs recovery delay after the PFG. Lock holding and gradient blanking are usually achieved incorporating appropriate commands into the pulse program. Experimental details describing some important practical matters such as checking for the presence of eddy currents, establishing proper refocusing condition, optimizing recovery delays and calibrating gradient strengths have been given[11,13] and will not be discussed here.
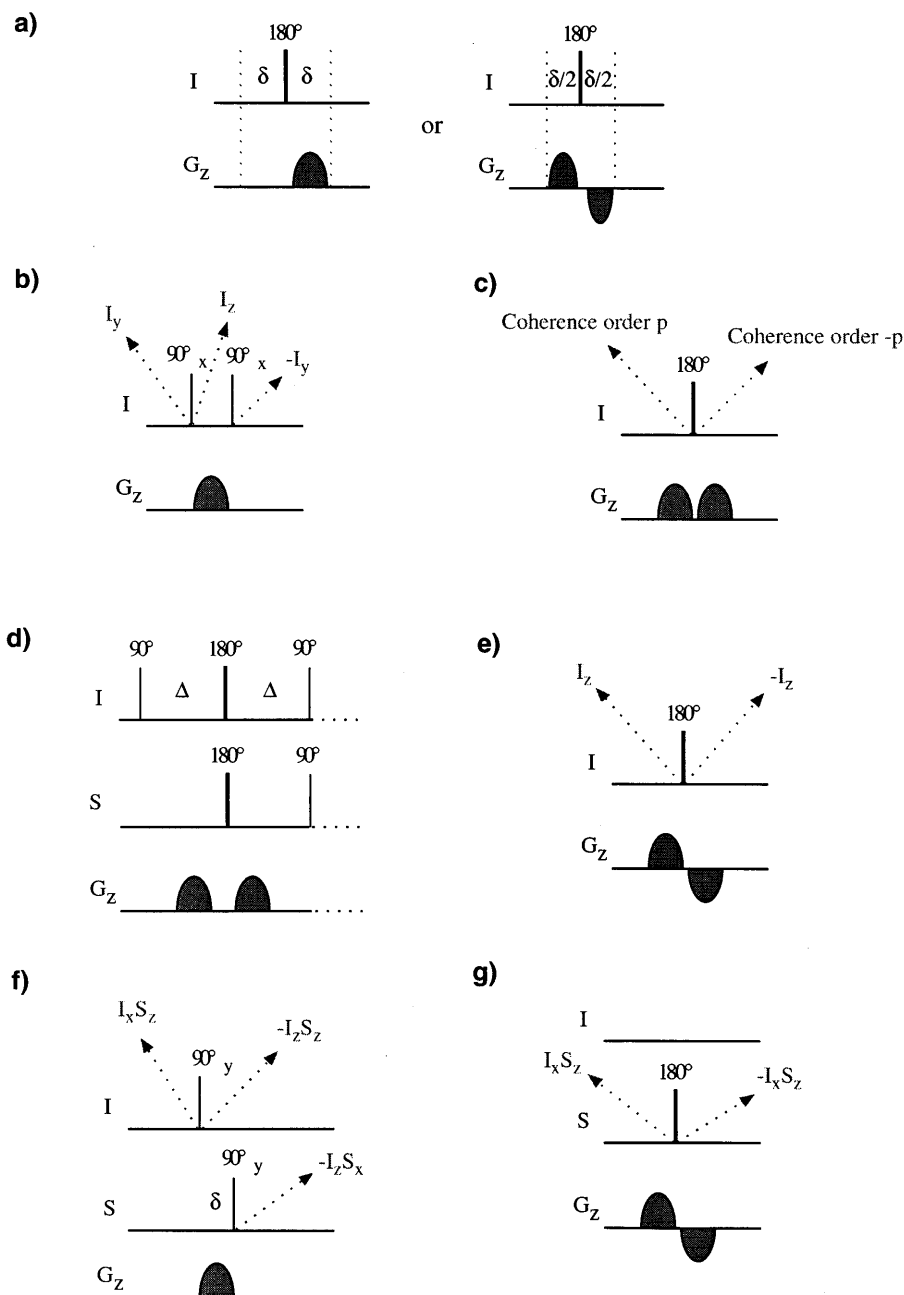
Figure 1. Useful building blocks incorporating PFGs into pulse sequences. The timings of the pulses and PFGs are represented in *I* (and *S* in heteronuclear cases) and G_z lines, respectively. Arrow annotations indicate the magnetization selected before or/and after each specific pulse. See the text for further discussion.

An important aspect for practical spectroscopists is the shimming procedure. Rapid high-quality automated shimming is now possible for both protonated[34] and deuterated solvents[35] using one and/or three-dimensional image-based field mapping. Without doubt, this technique affords a valuable tool for the full automation of data acquisition.

The consequences of gradient non-linearity on experiments employing diffusion weighting and magic-angle-gradient coherence selection have been discussed and methods to assess these effects and characterize gradient-coil performance have been presented.[36] On the other hand, the effects due to the use of PFGs together with trim pulses, the interference of back-ground gradients due to bad shimming with PFGs, and the residual eddy currents that cannot be completely compensated by adjustments of preemphasis, have been studied and methods for removing them have been proposed.[37] A theoretical study about the amount of residual transverse magnetization after the application of a PFG has been presented[38] and interesting aspects such as PFG orientation, sample dimensions, maximum strength and possible gradient imperfections have been studied and discussed in detail.

PFGs have been used during acquisition to suppress radiation damping and in order to study the effects of molecular diffusion on line broadening and lineshape for a *J*-coupled system.[39] On the other hand, radiation

damping can also be suppressed by applying bipolar PFG pulses in the evolution periods of homo- and heteronuclear nD experiments or applying a constant weak PFG during the mixing times in NOESY-type experiments.[40] Radiation damping can be also suppressed using gradient echoes during the delays of a DANTE pulse train selectively applied on the water resonance (the WANTED scheme)[41] without the need for extra hardware accessories.

The use of self-compensating PFG sequences ('PFG sandwich') has been proposed[42] in which a PFG is replaced by two PFGs, of half the duration and with opposite sign, placed either side of a 180° pulse. This approach allows for a great reduction in transient responses without tedious adjustments and without the need for additional hardware. Applications to measure the recovery time after the application of a PFG and the diffusion losses have been illustrated. The technique has been applied in 2D NOESY experiments,[43] 2D EXSY[44] and in DOSY applications.[45]

Spin-locking in an inhomogeneous B_0 or B_1 field gives near-perfect purging pulses which eliminate all magnetization which is not aligned with the spin-lock axis. Such purging pulses can also be used in the construction of high-quality z-filters without the need for stochastic variation of delays or phase cycling.[46] Examples of z-filtered TOCSY, NOESY and z-COSY experiments have been illustrated. On the other hand, systematic errors in the measurements of transverse relaxation times caused by oscillations due to a weak B_1 field can be removed by the application of a constant-gradient field during the CPMG period or by a series of PFGs flanking the reduced CPMG block.[47] The simultaneous use of pulses and PFGs has also been used to obtain homonuclear broadband decoupled NMR proton spectra.[48]

HOMONUCLEAR 2D EXPERIMENTS

In homonuclear experiments, the gyromagnetic ratio γ is the same for all spins and so Eqn (4) can be simplified to
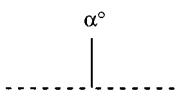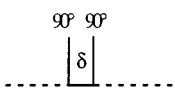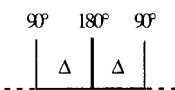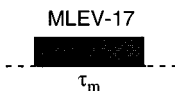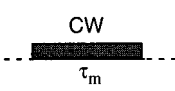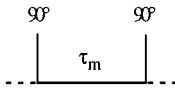
$$\sum_{i=1}^{n} p_i G_i = 0 \qquad (7)$$

The general scheme for recording homonuclear 2D experiments using gradients can be derived from the conventional phase-cycled scheme in which PFGs are placed just before and after the mixing process (Fig. 2). The nature of this mixing process will define the type of experiment to be recorded (see Table 1).

Assuming quadrature detection ($p_2 = -1$), the ratio between the two PFGs must be

$$p_1 G_1 - G_2 = 0 \qquad (8)$$

There are two possible solutions. If both PFGs are applied in the same sense ($G_1 = G_2$), the CTP corresponding to $p_1 = +1$ is selected (the continuous line in the CTP of Fig. 2); this results in echo or N-type data. On the other hand, if the gradients are applied in the opposite sense ($G_1 = G_2$) we select the coherence $p_1 =$

Table 1. Basic schemes for typical homonuclear mixing processes[a]

Experiment	Mixing	Effective Transfer
COSY	$\alpha°$	$I_{1x}I_{2z} \xrightarrow{J_{12}} I_{1z}I_{2x}$
COSY-MQF	90° δ 90°	$I_{1x}I_{2z} \xrightarrow{J_{12}} I_{1z}I_{2x}$
RELAY	90° Δ 180° Δ 90°	$I_{1x}I_{2z} \xrightarrow{J_{12}} I_{1z}I_{2x} \xrightarrow{J_{23}} I_{2z}I_{3x} \xrightarrow{J_{34}} I_{3z}I_{4x}$
TOCSY	MLEV-17 τ_m	$I_{1x} \xrightarrow{J_{12}} I_{2x} \xrightarrow{J_{23}} I_{3x} \xrightarrow{J_{34}} I_{4x}$
ROESY	CW τ_m	$I_{1x} \xrightarrow{ROE} I_{2x}$
NOESY	90° τ_m 90°	$I_{1z} \xrightarrow{NOE} I_{2z}$

[a] In the TOCSY scheme, other pulse trains such as DIPSI or WALTZ can also be used. In the ROESY scheme, a pulse train consisting of phase alternate 180° pulses (T-ROESY) can be applied. Finally, in NOESY experiments, a purge or homospoil gradient is usually applied during the mixing time.
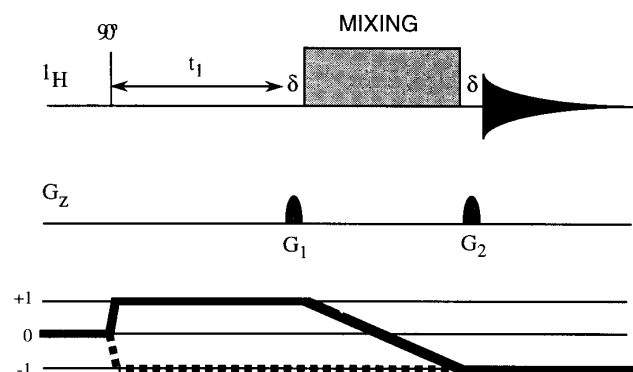
Figure 2. General scheme and coherence transfer pathways (CTP) for recording magnitude-mode gradient-based homonuclear 2D experiments. See Table 1 for some possible homonuclear mixing processes.

-1 (the shaded line in the CTP of Fig. 2); this results in antiecho or P-type.

In both cases, acquiring a single transient per t_1 increment gives a 2D map with frequency discrimination in the F_1 dimension. For example, Fig. 3 shows the 2D magnitude-mode (A) COSY[23,49] [see pulse scheme in Fig. 4(a)], (B) one-step RELAY[50] and (C) and (D) TOCSY[51] spectra of sucrose each required in about

5 min. All these experiments allow, in different ways, the study of through-bond proton–proton interactions via the J_{HH} coupling constant. Weaker long-range $^4J_{HH}$ and $^5J_{HH}$ proton–proton connectivities have been observed in COSY spectra of oligosaccharides using long, weak gradients; this is equivalent to a delayed-COSY experiment optimized to observe small couplings.[52] In addition to the substantial reduction of t_1 noise found in gradient-based experiments, the use of corrective data processing techniques such as reference deconvolution have been shown to reduce t_1 noise dramatically by an extra factor of 60 in a COSY experiment, allowing the observation of very small long-range correlations.[53] This approach is also applicable to other experiments. On the other hand, the effect of t_1 noise in P-type or N-type data acquisition has been evaluated in the COSY experiment.[54]

A simple variant of the COSY experiment has been used to observe surprising intermolecular multiple-quantum coherences in solution with at least one concentrated component.[55–58] In this, the so-called CRAZED experiment, the two PFGs around the second r.f. pulse are set to a $1:n$ ratio in order to select n-quantum coherences. This experiment leads to observable multiple-quantum transitions in the F_1 dimension
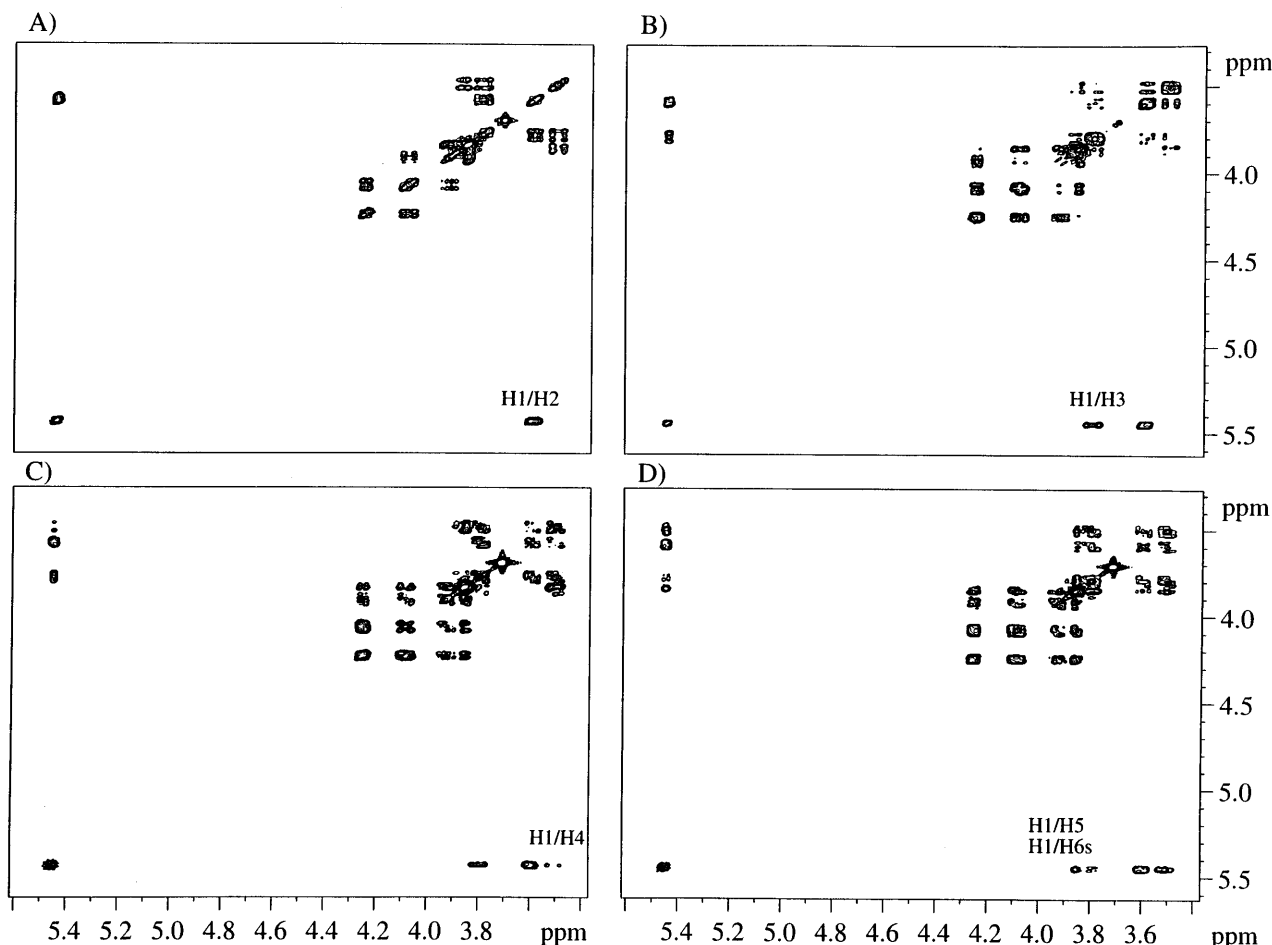

Figure 3. Magnitude-mode (A) 2D COSY, (B) 2D one-step RELAY (defocusing delay of 30 ms) and (C) and (D) 2D TOCSY spectra (40 and 120 ms of mixing, respectively) of 0.1 M sucrose in D_2O. A single scan for each 256 t_1 increment was recorded in each spectrum. Two sine-shaped gradients of the same duration (1 ms) and the same intensity (5 G cm^{-1}) were used in all cases. The total experimental time for each spectrum was about 5 min.
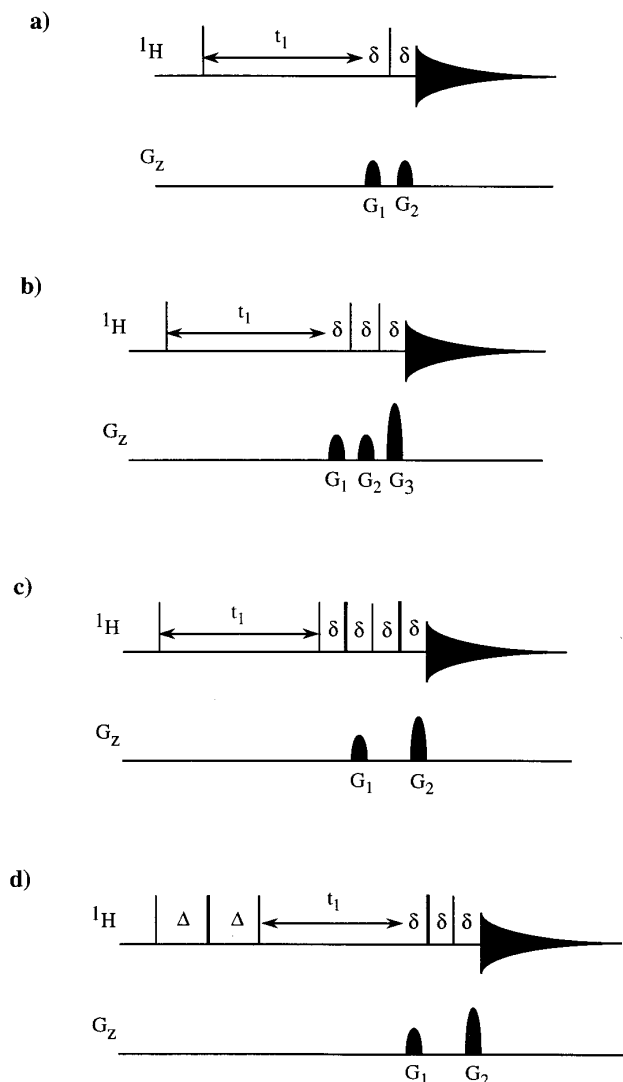
Figure 4. Pulse sequences for recording (a) 2D magnitude-mode COSY (gradient ratio 1:1, (b) 2D magnitude-mode MQF-COSY (gradient-ratio 4:3:10 for DQF and 1:1:4 for TQF experiments), (c) 2D phase-sensitive MQF-COSY experiments (gradient ratio 1:n) and (d) absolute-mode 2D multiple-quantum experiment (gradient ratio 1:n). Narrow and wide bars represent 90° and 180° pulses, respectively. The phase of all pulses is x unless indicated otherwise. δ is the gradient length and Δ is optimized to $1/4J_{HH}$.

and SQC in the directly detected F_2 dimension. The origin of these somewhat unexpected results have been extensively studied and discussed by several groups.[59-68]

The most widely used version of the 2D COSY experiment incorporates a multiple-quantum filter (MQF), consisting of the mixing 90°–PFG–90° block[49,51,69] [Fig. 4(b)]. In principle, a 1:1:(n + 1) gradient ratio was proposed to achieve proper n-filtering selection but recently it has been shown that a 4:3:10 gradient combination removes rapid-pulsing artefacts characteristic of magnitude-mode DQF-COSY experiments.[70] Alternatively, phase-sensitive MQF-COSY spectra can be obtained using the echo–antiecho approach[71] or avoiding the application of the defo-

cusing PFG during the variable t_1 period[69] [Fig. 4(c)]. Gradient-selected E. COSY spectra can be obtained combining several MQF-COSY spectra.[72]

In principle, PFGs are an effective method of suppressing the intense water resonance in aqueous solutions without the need for a selective perturbation to the water. However, it can sometimes be useful to combine this rejection procedure with some solvent suppression method. For instance, modified pure absorption 2D DQF-COSY experiments with improved water suppression using crafted selective pulses,[73] WATERGATE,[74] magic-angle gradients,[75,76] WET[77] and RAWSCUBA[78] schemes have been applied to samples dissolved in H_2O.

On the other hand, 2D NOESY and 2D ROESY experiments cannot be acquired using the scheme in Fig. 2 owing to the need for phase-sensitive presentation. Some possible alternatives use the echo–antiecho approach,[79] a strong spin-lock or a z-filter pulse prior to acquisition.[43,44,79] These approaches can also be applied to record phase-sensitive TOCSY spectra.[79] Recently, the application of a low-intensity gradient during the entire mixing period in a regular NOESY experiment, allowing the phase cycle to be reduced to two scans per t_1 increment,[80] has been proposed. In this case, 2D NOESY maps can be quickly obtained for concentrated samples in reduced times without unwanted sensitivity losses due to coherence selection and diffusion effects (Fig. 5). Recently, a modified NOESY pulse sequence has been proposed to suppress diagonal signals. In this way, NOEs between protons having similar chemical shift can be observed.[81] The NOESY pulse sequence can also be used to study dynamic or chemical exchange processes (termed EXSY experiment).[44,82,83]

There is also a set of homonuclear 2D experiments based on the creation and evolution of multiple-quantum coherences (MQC) that can be used as an alternative to the previously mentioned experiments. These experiments, known as zero-quantum (ZQ) and double-quantum (DQ) experiments [Fig. 4(d)], were pioneering experiments in high-resolution NMR spectroscopy and have been widely applied *in vivo* studies.[84-89] Analogous 1D MQ experiments have been also used for the same purpose.[88-91] On the other hand, 2D DQ experiments have recently been optimized to study large biomolecules in aqueous samples.[92-98] Thus, magic angle gradients have been successfully applied for effective suppression of the H_2O signal,[92] of multiple-solvent signals,[94] of solvent–solute DQC[93,94] and of radiation damping effects[93] in 2D DQ experiments. Alternatively, efficient suppression of radiation damping effects and the solvent signal can also be achieved using only a z-gradient.[97] Analogous 2D and 3D DQ-NOESY and DQ-TOCSY,[95] and 3D NOESY-DQ and TOCSY-DQ[96] experiments have been proposed to simplify proton resonance assignment of unlabeled biomolecules. A related approach has been used to explore dipole–dipole cross-correlations along an effective axis.[99]
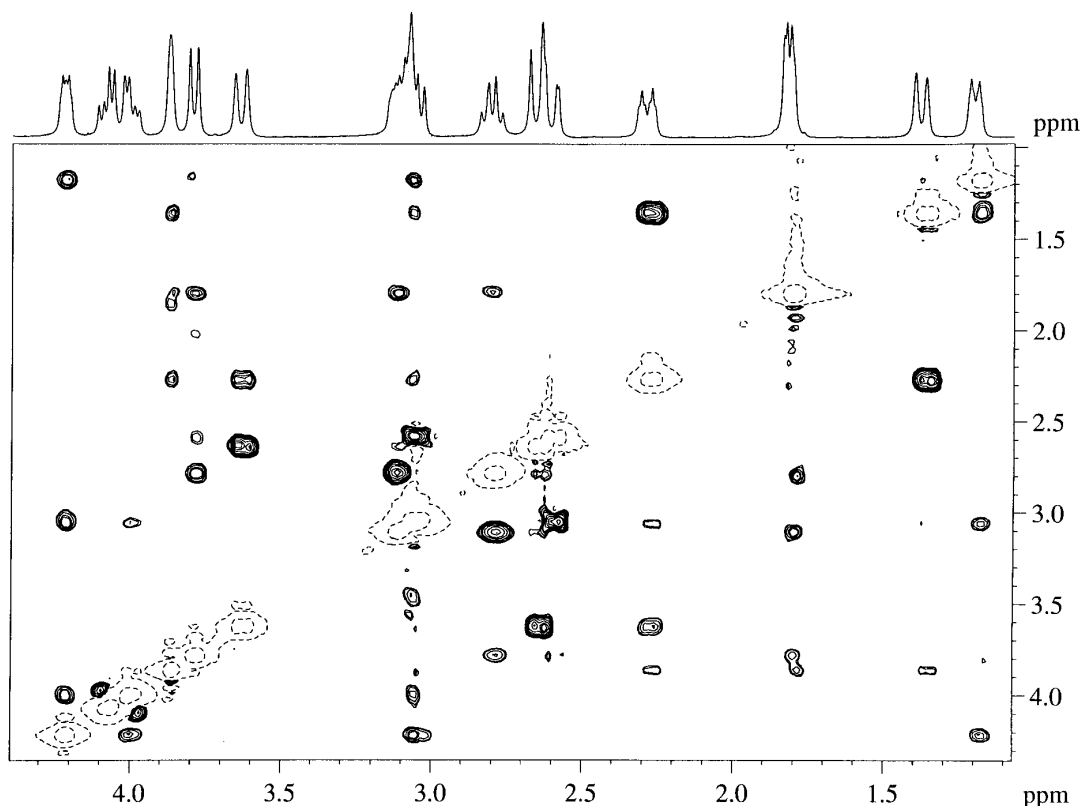
Figure 5. 2D NOESY spectrum of 0.1 M strychnine (mixing time 400 ms) in CDCl$_3$. Two scans per t_1 increment were recorded using the pulse sequence in Ref. 80, giving a total experimental time of 12 min. The phase of the first 90° pulse and the receiver were inverted on alternate scans. A single sine-shaped gradient of 400 ms was applied during the mixing time with a strength of 0.5 G cm^{-1}.

The DQ experiment has also been applied in 1D and 2D homonuclear studies of ^{13}C (carbon-detected INADEQUATE experiments)[100] although high sample concentrations are needed. An improved INADEQUATE-CR experiment doubles the sensitivity compared with the conventional experiments.[101–103] For practical purposes, better sensitivity can be achieved using analogous proton-detected experiments that will be discussed later.

2D HETERONUCLEAR EXPERIMENTS

Heteronuclear experiments based on proton detection are much improved by the use of gradients. The main inconvenience of this so-called inverse spectroscopy is the suppression of unwanted magnetization arising from ^{1}H–^{12}C (or ^{1}H–^{14}N), which is usually much more intense than the desired magnetization (^{1}H–^{13}C or ^{1}H–^{15}N). In the phase-cycled versions some elements are included to achieve this suppression such as, for instance, the BIRD-τ_{eff}(null) block in HMQC-type experiments[104] and the use of strong B_1 spin-lock periods in HSQC-type experiments.[105] However, t_1 noise often makes the spectral analysis difficult. Using gradients, these extra elements are not needed and the suppression of unwanted signals can be considered perfect.[106]

Both HMQC and HSQC pulse trains have been extensively modified to record gradient-based magnitude mode and pure absorption spectra under different conditions. However, an important aspect when PFGs are incorporated in such inverse experiments are the previously mentioned requirements of sensitivity and resolution. The sensitivity of several gradient-based HSQC and other related schemes has been extensively discussed.[29,30,107–111] It is possible, for instance, to design six different basic versions of the 2D ^{1}H–X HSQC experiments using PFGs. Which version is appropriate will depend on the sample under study.

1. The dephasing gradient G_1 is applied into the variable t_1 period [Fig. 6(a)], resulting in a magnitude mode spectrum.[112,113] This is an excellent option for routine samples in which sensitivity and resolution are not critical. In this case, the gradient ratio must satisfy the relationship

$$p_1\gamma_X G_1 - \gamma_H G_2 = 0 \qquad (9)$$

In the case when X = ^{13}C, we obtain $\gamma_H/\gamma_C \approx 4$,

$$p_1 G_1 - 4G_2 = 0 \qquad (10)$$

and two gradients with a 4:1 ratio select N-type data [continuous line in Fig. 6(a) corresponding to a $p_1 = +1$] whereas a 4: -1 ratio would select P-type data (dashed line corresponding to a $p_1 = -1$).

2. The echo–antiecho version of this experiment uses the same sequence as in Fig. 6(a), but the intensity of the
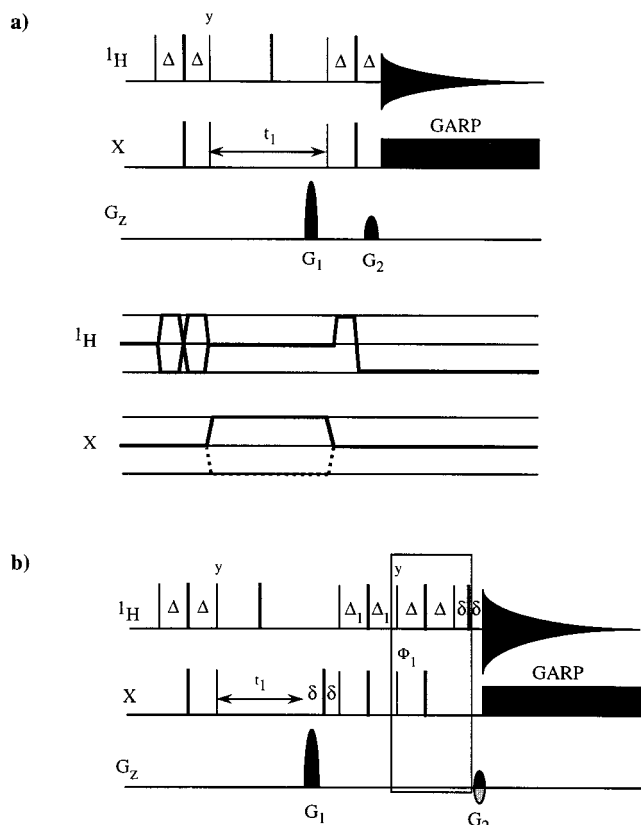
Figure 6. Pulse sequences for recording 2D HSQC experiments: (a) conventional scheme to obtain magnitude spectra and (b) pure-absorption scheme based on the echo–antiecho approach. The pulses and delays included in the frame stands for the optional sensitivity-improved version based on PEP methodology. Delays: Δ is set to $1/4^1J_{CH}$, δ is the gradient length and Δ_1 is optimized according to the carbon multiplicity. See the text and Table 2 for further details. The phase of all pulses is x unless indicated otherwise ($\phi_1 = x$). The phase ϕ_1 and the gradient G_2 are inverted in alternate scans and the corresponding data are stored separately and combined as discussed in the text.

approach, but the pulse sequence must be modified by adding a second reverse INEPT block in order to select both orthogonal components of the magnetization (I_zS_x and I_zS_y) present during t_1 [Fig. 6(b)]. As an example Fig. 7(A) shows the 2D HSQC spectrum of a 0.1 M strychnine sample acquired in 5 min. This basic scheme is widely applied to improve the sensitivity in other related multidimensional experiments.[29,30,109–111] Table 2 summarizes the theoretical enhancement factors of this experiment as a function of the Δ_1 optimization. However, some problems of this approach when applied to large biomolecules are as follows: (1) a larger number of pulses is required (the signal may be lost owing to r.f.
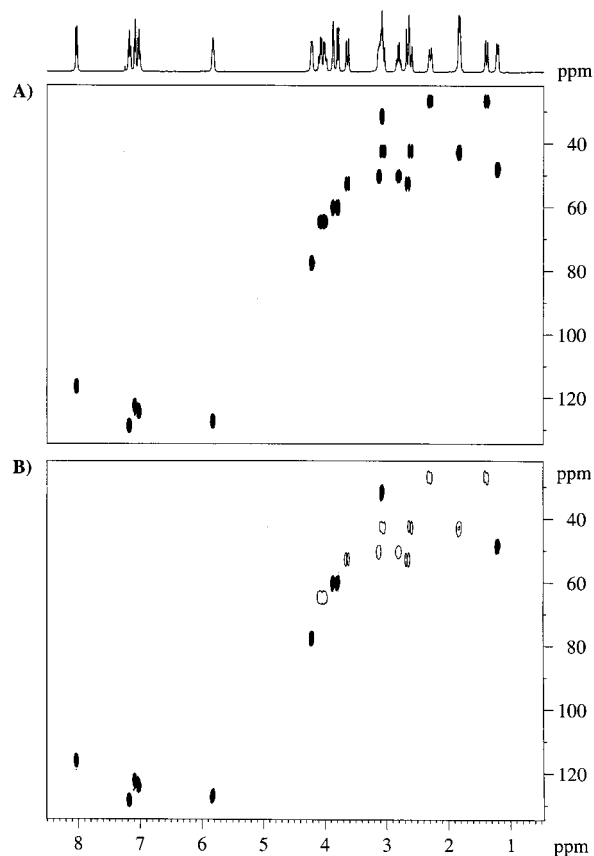
refocusing gradient G_2 is inverted on alternated scans to record the N- and P-type data separately.[24,114] After appropriate processing, phase-sensitive spectra are obtained but with a sensitivity loss by a factor of $2^{1/2}$ with respect to the phase-cycled experiment (Table 2).

3. Use of the PEP methodology[26–28] is the best option to record phase-sensitive 2D HSQC spectra with maximum sensitivity.[115] The selection procedure use the same principles as described for the echo–antiecho

Figure 7. Phase-sensitive 2D ^{1}H–^{13}C HSQC spectra of 0.1 M strychnine acquired with the pulse sequences described in (A) Fig. 6(b) and Fig. 8(c), respectively. Two transients were acquired for each 128 t_1 increments. In (B) filled cross peaks represent positive peaks belonging to methine systems and empty cross peaks represent negative methylene cross peaks.

Table 2. Theoretical enhancement factors obtained from several gradient-based HSQC experiments as a function of carbon multiplicities.

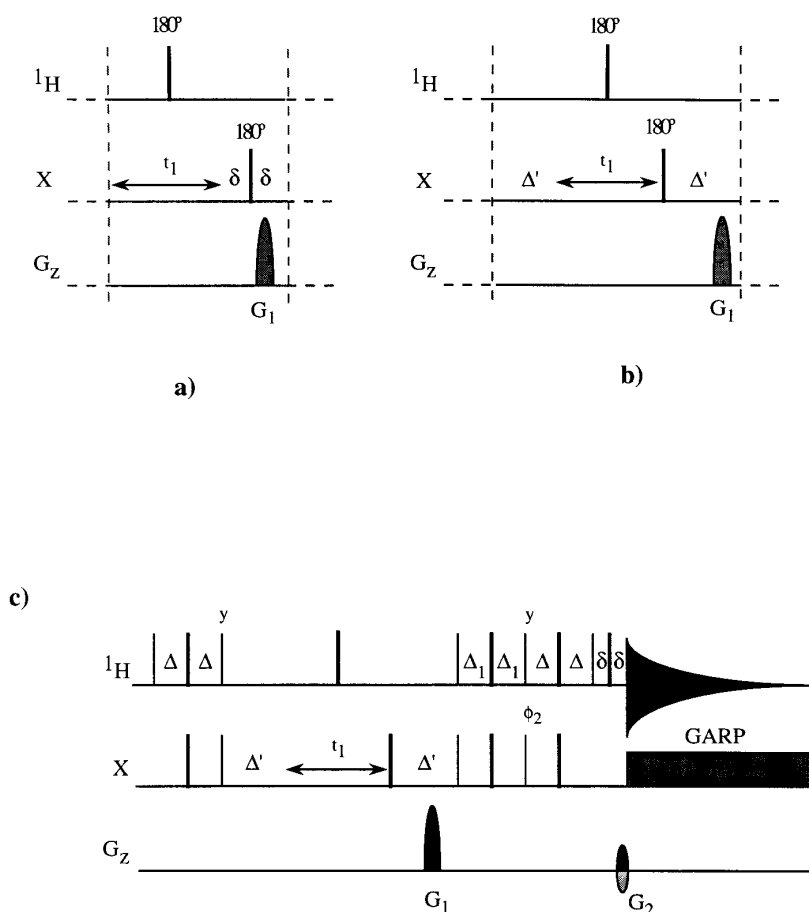| Experiment	IS	I_2S	I_2S	Δ_1
Echo–antiecho	0.707	1.414	2.12	
Phase-cycle	1	2	3	
PEP	1.414	1.414	2.12	$1/2J$
	1.20	2	2.54	$1/4J$
	1.06	1.92	2.65	$1/6J$

Figure 8. (a) Basic building block found in gradient-based ^1H–X HSQC-type experiments; (b) general building block to introduce X-multiplicity information in gradient-based ^1H–X HSQC-type experiments; (c) pulse scheme to record multiplicity-edited 2D ^1H–X HSQC experiments with improved sensitivity. The delays are optimized to $\Delta' = 2\Delta = 1/2'J_{CH}$ and Δ_1 is set as described in Table 2. Other acquisition and processing parameters as usually used for the HSQC experiment are described in Fig. 6(b).

inhomogeneity); (ii) the sequence is longer (the signal may be lost due owing to transverse relaxation); (iii) the sequence cannot be simultaneously optimized for all multiplicities; and (iv) there can be losses due to translational diffusion between PFGs. In triple resonance experiments applied to labeled proteins, the sensitivity can be further enhanced by simultaneous acquisition.[116] Some examples of modified PEP-HSQC experiments have been described to measure accurate $^1J_{NH}$,[117,118] measure a set of relaxation parameters in ^{15}N–^1H spin systems[119,120] or to observe exchange broadened signals.[121]

4. A z-filter, consisting of a $90°(X)$–PFG(δ)–$90°(X)$ block, is applied between the t_1 period and the dephasing G_1 gradient.[122] A phase-sensitive spectrum is obtained using the usual acquisition and processing procedures (e.g. TPPI), but there is a theoretical sensitivity loss of a factor of two compared to the phase-cycled experiment. However, this loss can be partially recovered applying the PEP methodology (a second reverse INEPT block shifted $90°$ in-phase)[123] without the need to apply the echo–antiecho approach.[124]

5. PFGs can be used as purge elements in the original phase-cycled sequence. These PFGs are placed between the simultaneous $90°$ pulses of ^1H and X in order to select the corresponding I_zS_z magnetization.[125,126] Although this is not a pure selection procedure, this approach reduces the number of phase cycle steps and minimizes artefacts due to poor suppression without affecting the overall sensitivity compared with that of analogous the phase-cycled experiment.

6. Much attention has been given to the effect of water suppression on the signal intensity of relatively rapidly exchanging protons, such as the NH protons in proteins. As a general approach, the WATERGATE block[127,128] is usually applied during the retro-INEPT block of the standard HSQC pulse sequence in order to improve solvent suppression in aqueous samples. WATERGATE can also be combined with the water flip-back approach[129] which ensures that the water magnetization is little perturbed and oriented along the $+z$ axis during most of the experiment, especially just prior to acquisition, to minimize the saturation of water. This is commonly applied to proteins and nucleic acids dissolved in H_2O. Other related approaches have been proposed to avoid the saturation transfer from water in HSQC experiments.[120,130–133] A detailed description about how PFG can be used in triple-resonance experiments in such a way as to avoid any sensitivity losses due to exchange has been given.[134]
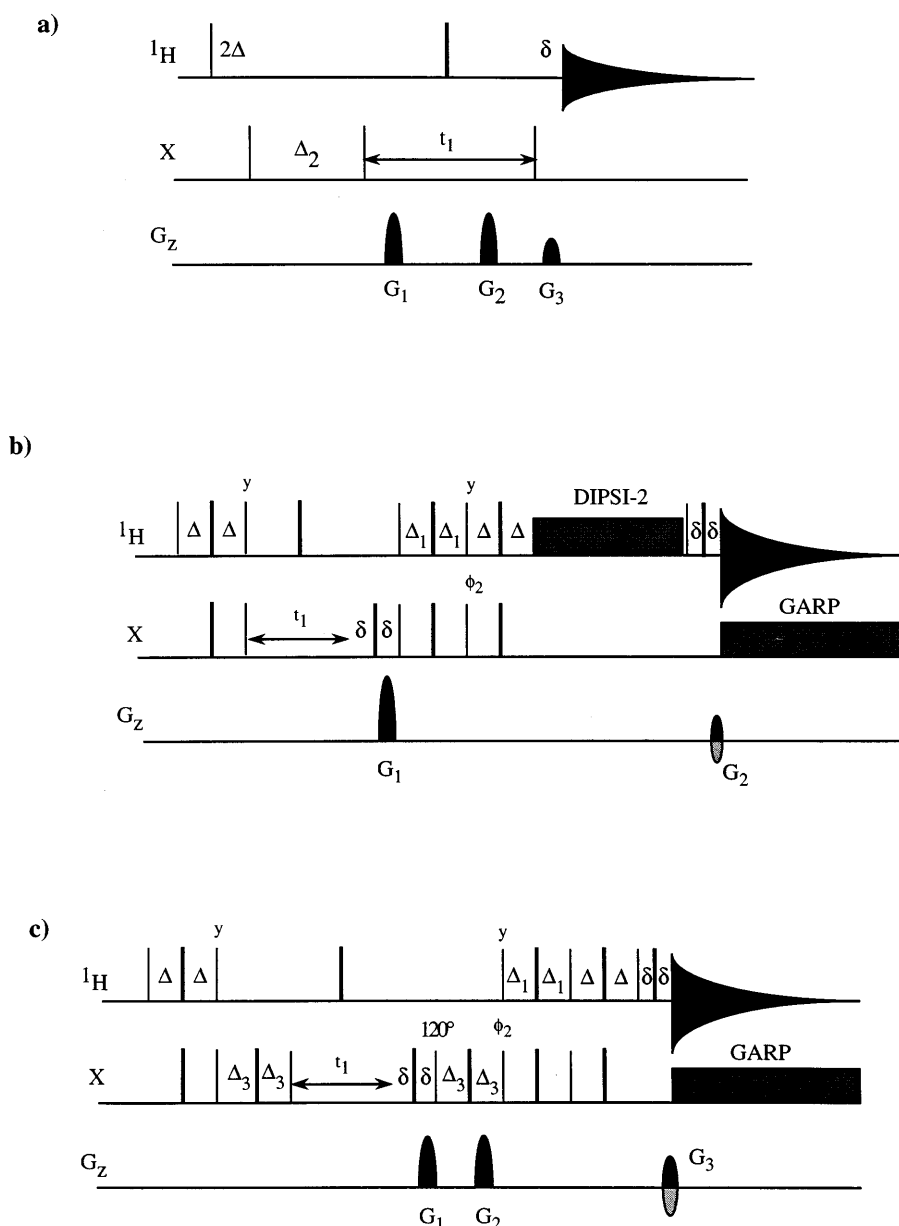
Figure 9. Pulse sequences for recording (a) magnitude-mode 2D HMBC (with an optional low-pass J filter, 2Δ), (b) sensitivity-improved pure-absorption 2D HSQC-TOCSY and (c) 2D 1,1-ADEQUATE experiments. Delay optimization: $\Delta = 1/4^1J_{CH}$, $\Delta_2 = 1/2^nJ_{CH}$, $\Delta_3 = 1/4^1J_{CC}$, δ is the gradient length and Δ_1 is optimized according to the multiplicity (see Table 2). Spectra derived from (b) and (c) are acquired and processed using the echo–antiecho approach.

In the same way as discussed for the HSQC experiment, 2D magnitude-mode HMQC experiment[106,112,113,135] and 2D phase-sensitive HMQC experiments, using the echo–antiecho approach[24,114,136,137] or incorporating a z-filter,[122,138] have been proposed. Phase sensitive HMQC experiments using diffusion filters in the defocusing–refocusing periods[139] and modified versions for recording in inhomogeneous fields[140] have also been described.

Multiplicity-edited HSQC experiment

A very important experiment for chemists is a multiplicity-edited heteronuclear correlation in which the multiplicity information of X nuclei is directly

obtained as additional information in the heteronuclear correlation map. In principle, this extra information can be introduced in any HSQC scheme giving pure absorption data[122] but, of course, the maximum sensitivity is obtained by a simple modification of the above described HSQC-PEP experiment [Fig. 8(c)].[141,142] In HSQC experiments, the dephasing gradient G_1 is usually placed into a carbon spin-echo, δ–180°(X)–G(δ), at the end of the t_1 period in order to avoid the evolution of offsets and couplings during the gradient [Fig. 8(a)]. If this block is substituted by a Δ'–180°(X)/Φ°(^{1}H)–Δ' block ($\Delta' = 1/2^1J_{CH}$), an X-signal intensity dependence of $\cos^{n-1}\Phi$ appears for an H_nX system.[141] In the more general approach, Φ is set to 180° and, therefore, a concatenated building block can be derived that avoids the application of an extra proton 180 pulse

[Fig. 8(b)].[42] For instance, Fig. 7(b) shows the 2D ^1H–^{13}C multiplicity-edited HSQC-PEP of strychnine recorded under the same experimental conditions as in Fig. 7(a). It can be observed that with a single experiment, the multiplicity of each carbon resonance is additionally displayed in the otherwise conventional HSQC spectrum and, therefore, all laboratories equipped with gradient capabilities can avoid the need for recording separate conventional DEPT and HSQC spectra to obtain this information. This same building block can be successfully incorporated in any multi-dimensional HSQC-type experiment,[142] as will be shown later.

Other editing approaches have been proposed from which two-dimensional I_nS-edited COSY,[43] TOCSY,[143,144] NOESY,[143] homonuclear J-resolved[145] and heteronuclear correlation[134,146] spectra can be obtained. In all these experiments PFGs are used to select specific n-quantum coherences that can simplify the analysis of highly overlapped spectra, although sensitivity losses are unavoidable due to coherence selection.

HMBC experiment

The HMBC experiment is another experiment that greatly benefits from the application of gradients.[106] High-quality spectra without subtraction artefacts are usually obtained in standard conditions, allowing the analysis of even very tiny, but informative cross peaks. The pulse sequence is basically derived from the HMQC pulse train in which an optional low-pass J-filter [2Δ–$90°(X)$, where $\Delta = 1/4^1J_{XH}$) can be inserted after the first pulse to minimize direct responses, the evolution period is optimized to an $1/2^nJ_{XH}$ value, and the refocusing period and the X decoupling during acquisition are removed [Fig. 9(a)]. PFGs are incorporated in the same way as the conventional HMQC experiment and the final spectrum is usually presented in magnitude mode in order to extract qualitatively heteronuclear long-range connectivities, mainly on quaternary carbons or through heteronuclei. Some variants have been proposed to improve sensitivity by using selective or semi-selective proton pulses which suppress ^1H–^1H J modulation and allow the correlation of poorly resolved proton multiplets,[147] to measure $^nJ_{CH}$ [148–150] and to minimize direct responses.[151] Practical applications on ^{15}N,[152–154] ^{31}P[155] and ^{119}Sn[156,157] have also been published. An analogous long-range optimized ^{31}P–^1H HSQC experiment has also been published.[158] As an example, Fig. 10 shows the magnitude-mode artefact-free ^1H–^{13}C and ^1H–^{15}N 2D HMBC spectra of strychnine without any further data post-processing.

Hybrid 2D experiments

A second generation of experiments are available that can give valuable structural information when the more conventional experiments do not resolve a particular
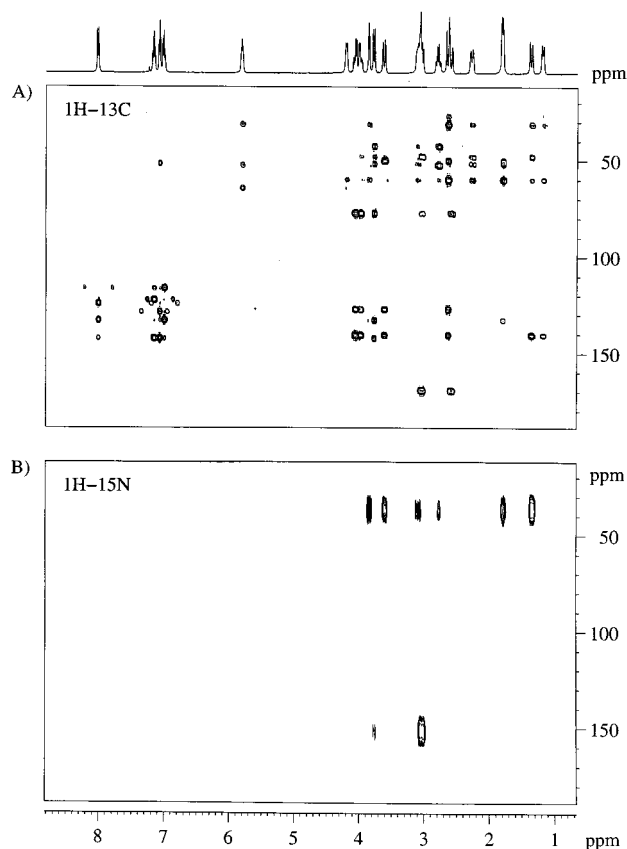

Figure 10. Magnitude-mode 2D (A) ^1H–^{13}C and (B) ^1H–^{15}N HMBC spectra of strychnine using a defocusing delay Δ_2 of 60 ms in both cases.

question. In particular, HMQC and HSQC pulse trains can be understood as equivalent building blocks in which the required input and output data are in-phase proton magnetization. In this way, both schemes can be combined with any homonuclear mixing process in order to design more sophisticated experiments. As an example, Fig. 11 shows the general scheme for such hybrid experiments using the echo–antiecho approach of the HSQC experiment. The gradient ratios should be exactly the same as discussed before (for instance, $4:1$ and $4: -1$ in alternate scans for X = ^{13}C).

Gradient-based sequences for the 2D HSQC-COSY, 2D HSQC-TOCSY, 2D HSQC-ROESY and 2D HSQC-NOESY experiments can be designed combining this general scheme and the mixing processes described in Table 1. For instance, related versions of multi-dimensional HMQC-COSY,[122,159] HMQC-TOCSY,[122,160,161] HSQC-TOCSY,[122,162a] HSQC-NOESY,[162b,163] NOESY-HMQC,[164–165] NOESY-HSQC[128,164,166,167] and TOCSY-HSQC[166] experiments have been proposed.

Special mention must be made of the gradient-based 2D HSQC-TOCSY experiment because, as discussed for the HSQC experiment, it is possible to incorporate the PEP methodology [Fig. 9(b)] into this experiment. In addition, the HSQC-TOCSY experiment can be acquired with several variants, depending on whether editing of direct responses or editing of X-nucleus multi-
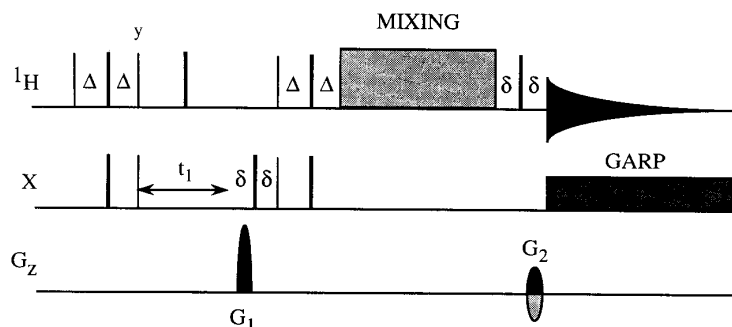
Figure 11. General scheme for recording pure-absorption 2D heteronuclear hybrid sequences using the echo–antiecho approach. See Table 1 for some useful homonuclear mixing processes and the text for further discussion.

plicity are included. Figure 12 shows several possibilities to obtain ^{1}H–^{13}C HSQC-TOCSY spectra on strychnine as a function of such editing capabilities: (A) a conventional 2D HSQC-TOCSY map using the pulse sequence in Fig 9(b) in which all cross peaks are in pure absorption, in-phase and with positive intensity; (B) direct correlations can be separated from the relay peaks by using an editing block just prior to acquisition; (C) carbon multiplicity information of the direct peaks is encoded using the building block described in Fig. 8(b)[142] giving positive peaks for methylenes and negative peaks for methines; (D) both editing blocks

can simultaneously be applied and, therefore, both forms of editing are present.

Another interesting hybrid experiment is an X-coupled 2D HSQC-NOESY experiment[162b] from which NOEs between chemically equivalent or accidentally overlapped protons (useful for the study of symmetrical molecules) can be detected.

Recently, a new set of ^{1}H-detected INADEQUATE-type experiments have been proposed to trace out heteronuclear connectivities combining the information on J_{CH} (HSQC or HMBC) and J_{CC} (INADEQUATE) coupling constants. Such experiments have been derived
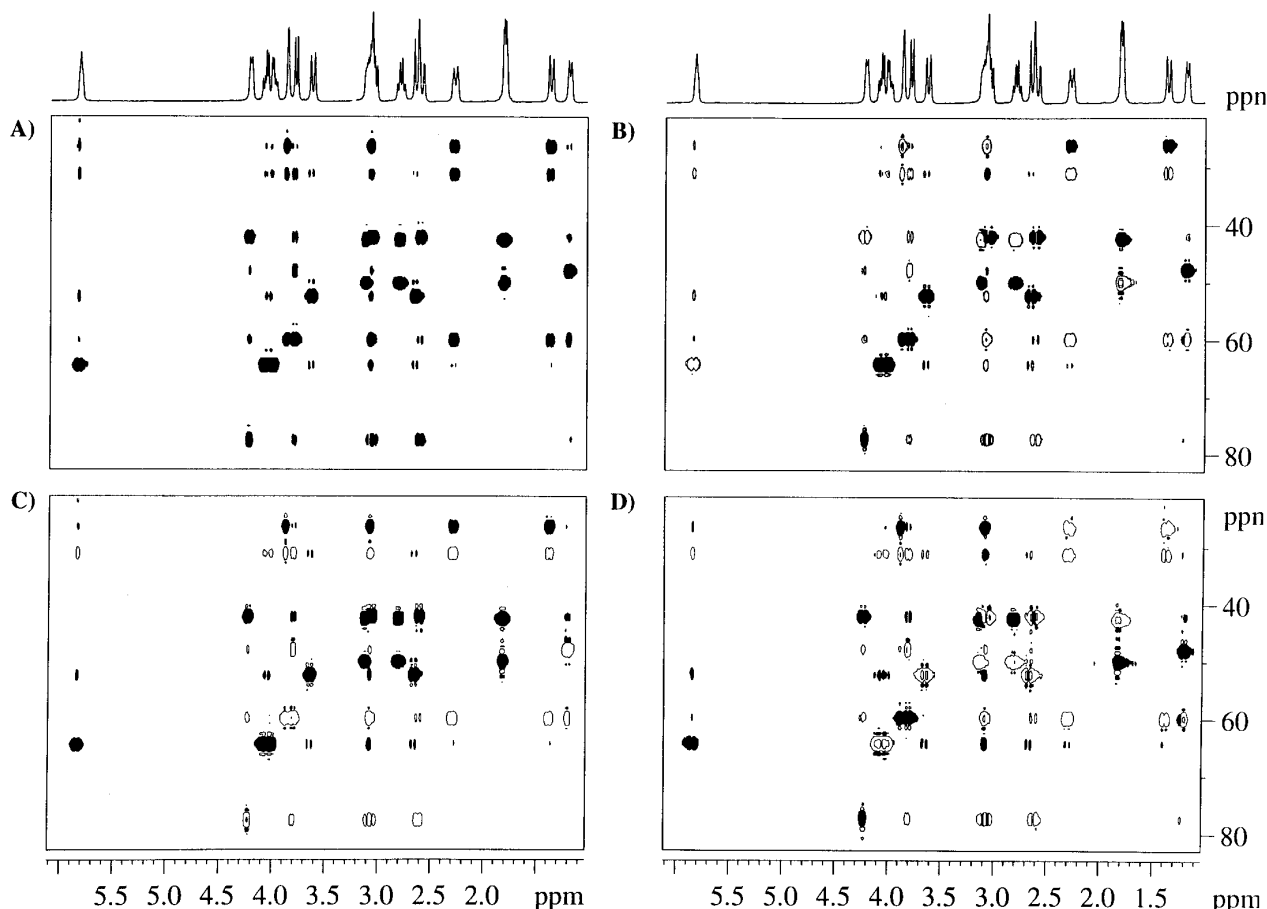

Figure 12. Sensitivity-improved 2D ^{1}H–^{13}C HSQC-TOCSY spectra of strychnine in CDCl$_3$: (A) conventional spectrum acquired with the pulse sequence of Fig. 9(b); (B) as (A) but incorporating editing of direct responses; (C) as (A) but incorporating editing of carbon multiplicity; (D) as (A) but incorporating editing of direct responses and multiplicity editing. Positive peaks are filled and negative peaks are empty. Further discussion is given in the text.

from the widely used 2D–4D HCCH-type experiments, commonly applied in ^{13}C-labeled proteins and nucleic acids. Examples are the reverse INEPT-INADEQUATE,[168] its ^{13}C-relayed variant,[169] carbon-displayed HMQC-INADEQUATE[170] and HSQC-INADEQUATE[171–173] and the sensitivity-improved ADEQUATE[174–176] experiments. Simple variants of these experiments have been used to assign and measure one-bond[177,178] and long-range[177,179] carbon–carbon coupling constants. Otherwise, long-range carbon–nitrogen coupling constants can be mea-

sured from a closely related triple-resonance experiment.[180]

For instance, the 1,1-ADEQUATE experiment[174] is an HSQC-PEP experiment in which the usual evolution period has been substituted for a period in which creation and evolution of ^{13}C–^{13}C double-quantum coherences take place [Fig. 9(c)], similar to the INADEQUATE experiment. A refocused version of this experiment would permit the differentiation of cross peaks arising from $^2J_{CH}$ and $^3J_{CH}$ in an HMBC spectrum.[175] Figure 13(A) shows the 1,1-ADEQUATE spec-
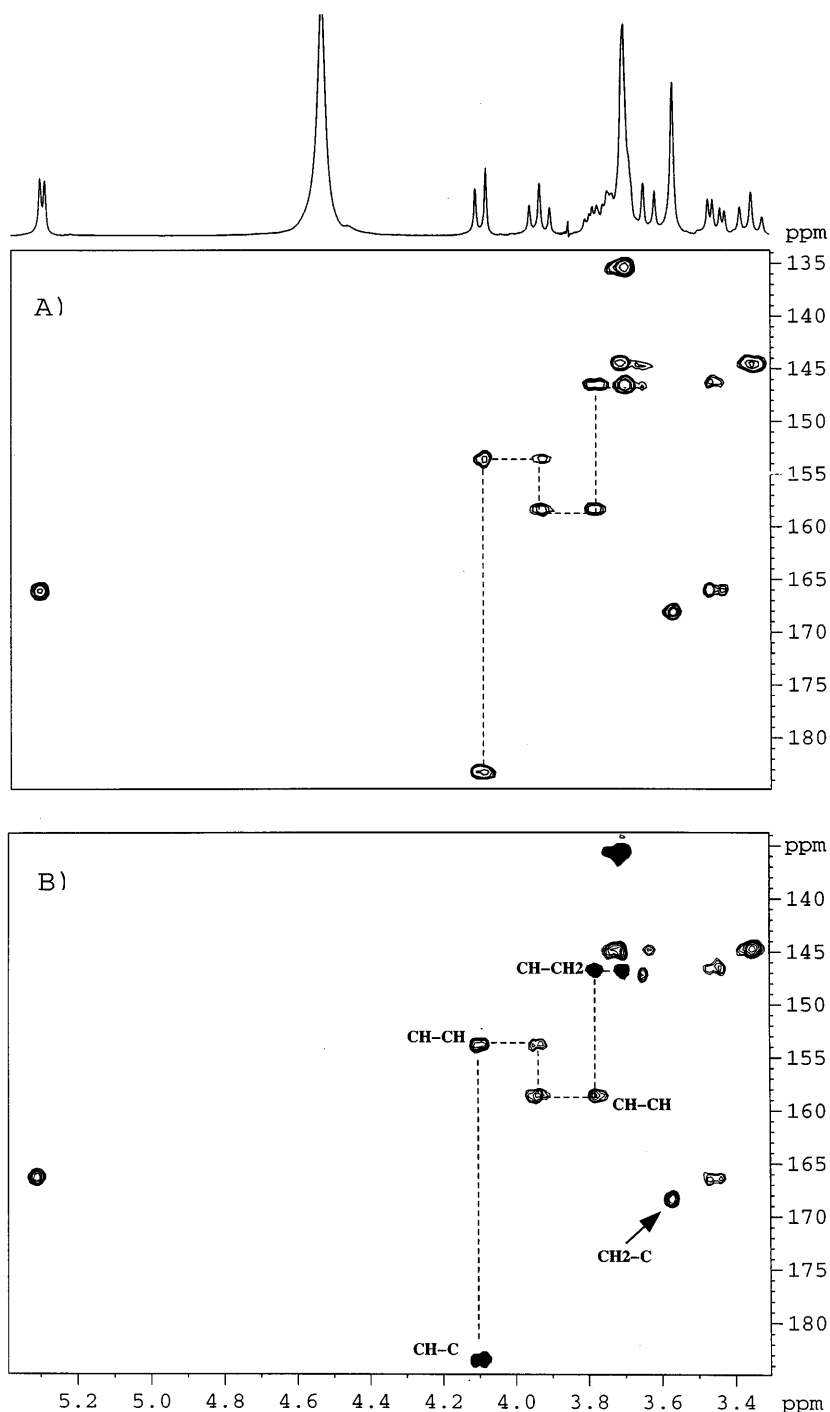

Figure 13. Pure absorption 1,1-ADEQUATE spectra of sucrose (A) without and (B) with multiplicity editing. Negative peaks are filled.
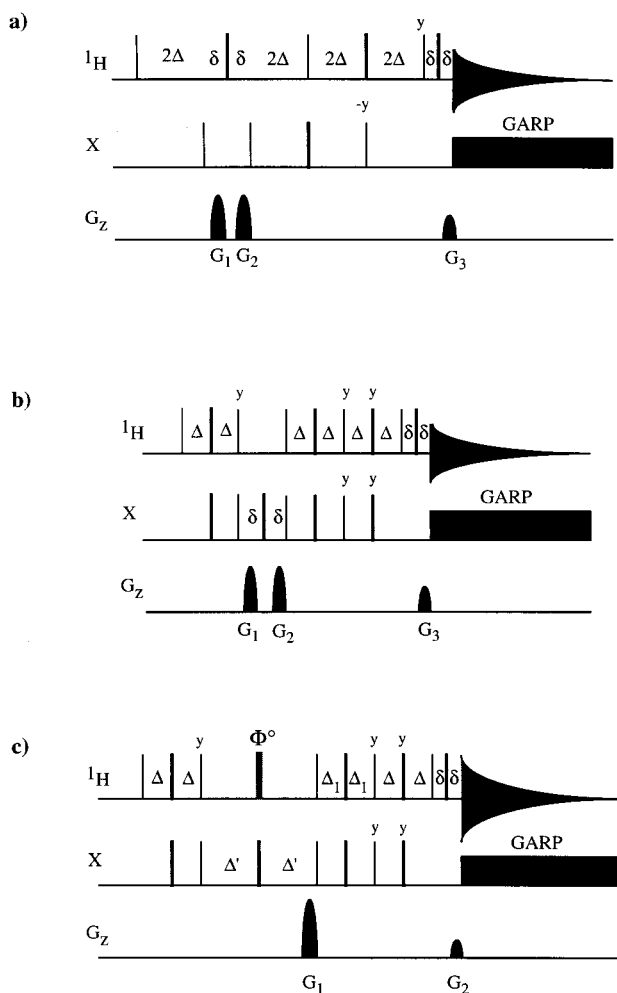
Figure 14. Pulse sequences to record gradient-based sensitivity-improved versions of the (a) 1D HMQC, (b) 1D HSQC and (c) 1D multiplicity-edited HSQC experiments. A minimum two-phase cycle was used in which the first 90° (X) pulse and the receiver are inverted on alternate scans. The gradient ratios for each experiments are 2:2:1, 2: − 2:1 and 4:1, respectively. Other acquisition parameters as described for their 2D analogs.

trum of sucrose acquired in about 2 h using the pulse sequence of Fig. 9(c). On the other hand, if the DQ evolution period is optimized to $^nJ_{CC}$, we would obtain the 1,n-ADEQUATE experiment that reveal heteronuclear correlations to three and four bonds. Similar results can be obtained from an n,1-ADEQUATE experiment ($^nJ_{CH} + {}^1J_{CC}$). Finally, from an n,n-ADEQUATE experiment ($^nJ_{CH} + {}^nJ_{CC}$) correlations up to six bonds can be obtained in a single spectrum. As discussed above, carbon multiplicity can be also included in ADEQUATE experiments[142] allowing the exact skeletal structure of C–C systems to be extracted. Thus, from a multiplicity-edited 1,1-ADEQUATE spectrum, CH–CH and C–CH$_2$ correlations are positive whereas C–CH and CH–CH$_2$ are negative. Observe in Fig. 13(B) how both the substructures of both residues of sucrose can be fully elucidated by simple spectral analysis.

Miscellaneous applications

Only applications between ^1H and ^{13}C have been described because of their wide interest in organic chemistry, but these experiments can be applied to any heteronucleus allowing the use of these techniques for organometallic and inorganic compounds. Two excellent reviews have appeared dealing with 2D chemical shift correlations between ^{13}C and other heteronuclei[181] and with all combinations of NMR active nuclei in the Periodic Table.[182,183] In principle, all proposed inverse schemes can be recorded using gradients in spectrometers equipped with three channels, in which we can apply similar experiments between two heteronuclei X,Y while decoupling ^1H. Some examples are the selective triple-resonance ^1H–^{13}C–^{31}P (SELTRIP) experiment[184] and the more sophisticated ^1H–^{13}C–^{31}P and ^1H–^{13}C–^{31}N experiments specifically designed to study nucleic acid derivatives.[185]
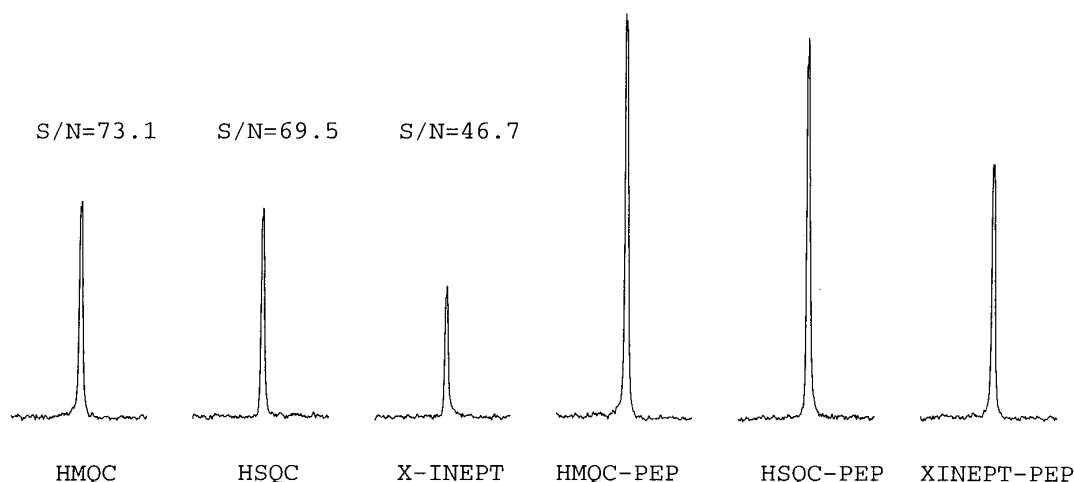

Figure 15. Experimental sensitivity enhancement factors due to the incorporation of PEP methodology in several 1D inverse experiments using PFG. The signal monitored is the H$_1$ proton of the sucrose after selectively pulsing its directly attached C$_1$ carbon. Both transmitter and decoupler offsets were applied on resonance. Eight scans preceded by two dummy scans were recorded for each spectrum and the data were processed using a 1 Hz line broadening.
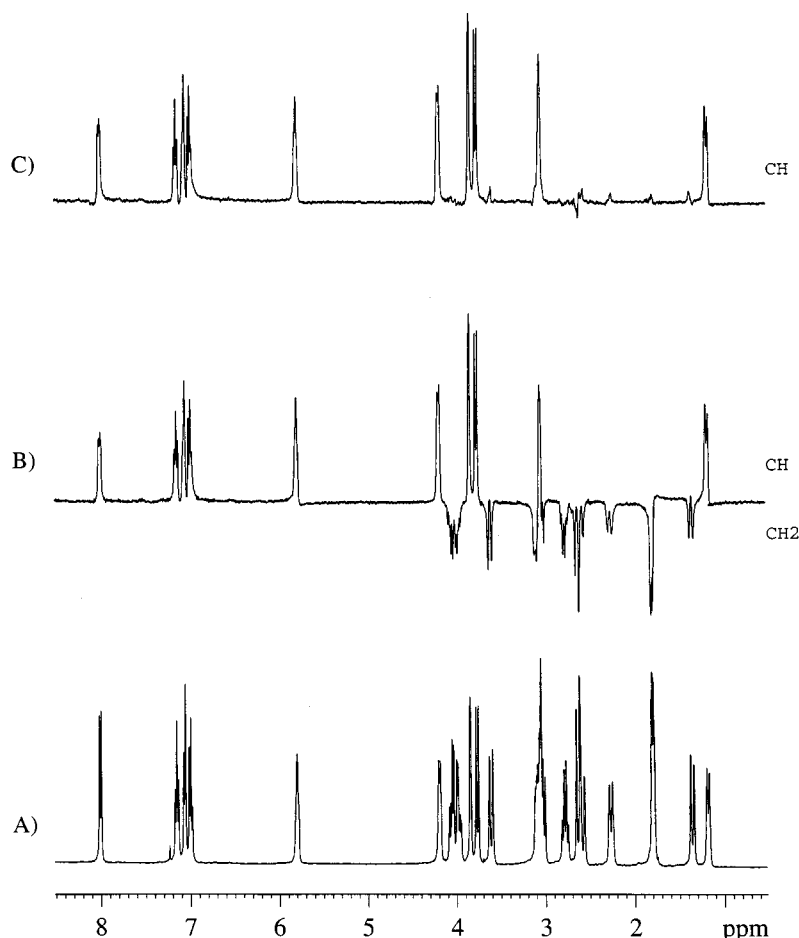
Figure 16. Sensitivity-improved multiplicity-edited 1D HSQC spectra of strychnine obtained from the pulse sequence in Fig. 14(c). (A) Conventional 1H spectrum; (B) and (C) multiplicity-edited spectra acquired with $\Phi = 180°$ and $90°$, respectively. Sixty-four scans preceded by four dummy scans were acquired for each spectrum. Data were processed using a 1 Hz line broadening.

Another interesting topic is the detection of heteronuclear NOEs on non-protonated X-nuclei using the gradient-enhanced proton-detected analog of the HOESY experiment, which has been successfully applied between ^1H, ^{31}P and ^1H, ^7Li nuclei.[186] In principle, the idea can be extrapolated to study ^{13}C but sensitivity is the inherent limiting factor.

A simple variant of the HSQC pulse sequence allows the measurement of direct and long-range proton–carbon coupling constants from a proton-detected J-resolved 2D spectrum. It is based on the application of a selective 180° proton pulse simultaneously with a hard 180° carbon pulse during the evolution t_1 period.[187] A heteronuclear J-resolved experiment, so-called ACT-J (an acronym for active coupling-pattern tilting), has been described to measure efficiently and assign heteronuclear coupling constants[188] and to acquire homonuclear and heteronuclear J spectra with pure phases, tilted cross peaks patterns and homonuclear I-spin decoupled signals in the F_1 dimension. Examples of such measurements of silicon–proton coupling constants are provided.[189,190] Recently, a novel approach that selectively excites resonances corresponding to exclusively either the α or β spin state of a coupled het-

eronuclear spin has been described and applied to measure coupling constants.[191–193]

Gradient-based isotope-filtered schemes have been proposed and incorporated in multi-dimensional experiments to allow the assignment of intermolecular NOEs between labeled and unlabeled molecules.[194–196]

INVERSE 1D EXPERIMENTS

PFGs can also be successfully applied in 1D analogs of the above discussed inverse 2D experiments. Illustrative examples are the application of gradient-based 1D HMQC experiment in *in vivo* studies,[197] in triple resonance applications[198] or to study organometallic compounds such as low-abundance ^{119}Sn nuclei.[156,157] In addition, the improved-sensitivity PEP methodology can be applied in inverse 1D experiments based on gradients in order to regain the sensitivity losses due to coherence selection.[199] Figure 14 shows the basic gradient-based sensitivity-improved 1D (a) ^1H–X HMQC and (b) HSQC pulse sequences. Extensions of such sequences can also be applied in, for instance, selective[200] or in triple-resonance X,Y$\{^1H\}$ analogs. The

major advantages of these approaches is that an increase in the signal-to-noise ratio by a factor of two is obtained, as theoretically predicted, when compared with the conventional versions. Figure 15 shows, as an example, the experimental enhancement factors found for the H_1–C_1 pair of sucrose (*IS* system) in selective versions of 1D HMQC, HSQC and X-INEPT experiments;[200] the improvements agree well with the theoretical predictions.

In a similar way, the multiplicity of I_nS systems can also be obtained from a proton spectrum acquired using the 1D analog of the edited-HSQC-PEP experiment [Fig. 14(c)]. Figure 16 shows the 1D multiplicity-edited HSQC-PEP spectra of strychnine[141] that offer information similar to the conventional DEPT spectra. Other 1D approaches to multiplicity editing by which suffer from sensitivity losses due to coherence selection have also been described.[146,201–203]

SELECTIVE SPIN ECHO

Currently, a very important element in high-resolution NMR methodology is the selective pulsed-field-gradient spin-echo (SPFGE) block. The general scheme is based on the initial creation of transverse magnetization followed by a inversion element (Fig. 17). Two gradients of the same duration and intensity are applied just before and after the inversion element, allowing the final refocusing of only the magnetization which experiences the inversion pulse; no phase cycling is needed.

As a function of the applied inversion element, we can distinguish three different applications:

1. When this element is a selective 180° pulse applied on a single resonance, we obtain a simple and very useful tool which achieves excellent selective excitation in a single scan. This can be used as a starting point in any selective 1D experiment.
2. When this element is a semi-selective pulse applied in a specific region of the spectrum, we obtain a general approach to semi-selective excitation. This can be
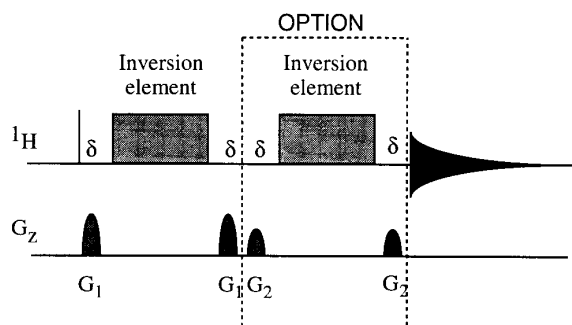
useful for improving resolution, reducing acquisition times or achieving selective decoupling (spectral simplification and improved sensitivity) in multi-dimensional experiments.

3. When this element is a 180° pulse for all resonances except one, we obtain a general approach to solvent suppression. It can be useful to record multi-dimensional homo- and heteronuclear spectra of biological samples in H_2O.

Applications of the SPFGE scheme have been demonstrated for effective solvent suppression in aqueous solutions (the WATERGATE scheme[127,128]), water-selective excitation to study solvent–solute interactions,[204–207] clean selective excitation in selective 1D homonuclear[208–213] and heteronuclear[162] experiments, multiple-signal excitation and multiple-solvent suppression[214] and band-selective excitation in semi-selective 2D and 3D experiments.[214–217] An accurate phase-sensitive method based on a gradient spin-echo sequence has been proposed for obtaining the excitation profile and the phase behavior of a shaped selective 90° and 180° pulse.[13,218]

An extended approach using a double pulsed-field-gradient spin echo (DPFGE), termed excitation sculpting, has recently been proposed as an improved alternative to achieve all these goals. A number of applications have also appeared, e.g. solvent suppression,[219,220] selective excitation,[221] selective 1D experiments,[222–225] carbon selective excitation,[226] multiple excitation,[227,228] multiple solvent suppression,[229,230] semi-selective excitation[231–233] and isotope editing (G-BIRD scheme).[234–236] Recently, a related G-BIRD scheme using r.f. gradients has been described.[237]

Selective excitation

The phase properties of the SPFGE experiment are closely related to the phase properties of the refocusing element. In contrast, the excitation profile of the DPFGE experiment depends only on the inversion profile of the refocusing pulse, while the amplitude is scaled both by the inversion profile of the refocusing pulse and by unavoidable losses due to relaxation during the spin echo. The main features in favor of the use of these gradient-based spin-echo schemes are as follows: (1) ultra-clean pure-absorption phase 1D spectra are simply obtained without frequency-dependent phase variations of the excited signal throughout the selected region; (ii) no presence of side-lobes and/or sidebands outside the effective bandwith; (iii) the full refocusing of all *J*-evolution at the end of the echo (only if one of the coupled partner is excited); (iv) the sequence is very tolerant to miscalibrated pulses and r.f. inhomogeneity; and (v) no phase cycling is required, thus avoiding the need for difference spectroscopy.

In practice, for instance, the use of a Gaussian-shaped inversion pulse in SPFGE and DPFGE schemes gives

Figure 17. Basic scheme for SPFGE and DPFGE experiments. The inversion element can be multiplet-selective or band-selective pulses for selective excitation or solvent suppression purposes. In the case of DPFGE scheme, the strength of G_1 must be different to that of G_2. Further discussion is given in the text.
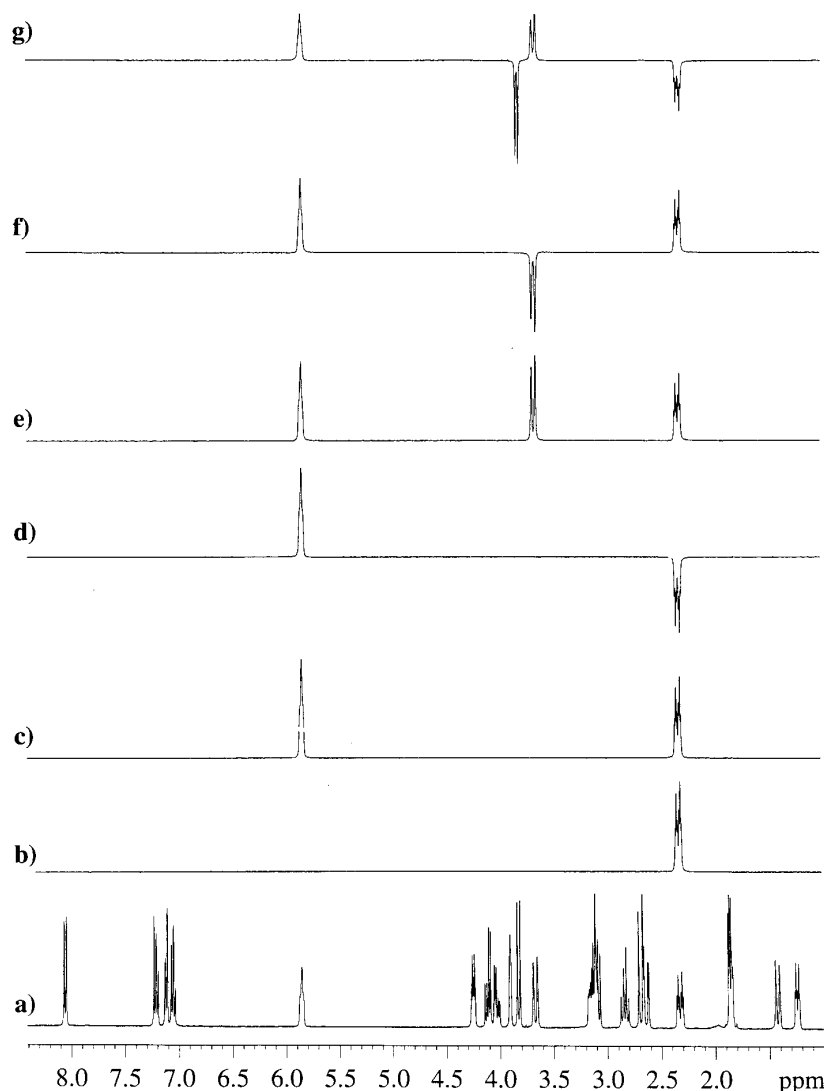
Figure 18. (a) Conventional 400 MHz spectrum of strychnine in $CDCl_3$, (b) single-site excitation with a 20 ms Gaussian 180° pulse and (d)–(g) multiple-site selective excitation using the DPFGE scheme. In the last case, the duration of each selective inversion pulse depends of the selectivity required. The relative phase of each excited signal depends solely on the phase of the corresponding selective pulse. A single scan was recorded for each spectrum.

excellent results in terms of selectivity, absence of side-lobes, lack of J-evolution and absence of phase errors in the desired region. Note the excellent experimental properties from the single-scan DPFGE spectrum after a selective pulse (20 ms, 5% truncated Gaussian) applied to the H-15 proton of strychnine [Fig. 18(b)]. A simple modification of this scheme, using concantenated selective pulses, can be successfully used to achieve multiple-site selective excitation under the same conditions as the original experiment.[215] Figure 18(c)–(g) show several examples of multiple-site excitation achieved in a single scan from which the selectivity and the phase of each selective excitation can be controlled with great simplicity.

The excellent general behavior of both SPFGE and DPFGE schemes is very useful when applied to selective homonuclear 1D experiments.[12,13] There are a number of reasons which favour the use of such selective 1D experiments rather than their 2D analogs; (i) 1D spectra allow a more reliable data analysis to be

made; (ii) increased digital resolution; (ii) reduced acquisition and processing times; (iv) minimum data storage requirements; (v) PFGs can sometimes be included without sensitivity losses; and (vi) highly useful when a limited amount of information is desired (this is a typical situation for small and medium-size molecules).

Figure 19 shows the general scheme to perform such experiments using PFGs. As a selective excitation we can use either the SPFGE or DPFGE block. After the mixing process (see Table 1) we have the option to apply a refocusing gradient G_3 just prior to acquisition. If G_3 is applied (in this case the sense of the second G_1 must be reversed) we obtain clean 1D spectra without the need for phase cycling but with a theoretical sensitivity loss by a factor of two when compared with an analogous phase-cycled experiment because of the selection of a specific CTP. If G_3 is not applied, we need to apply a basic four-step cycle (EXORCYCLE)[238] on one of the 180° selective pulses but, in this case, there are no
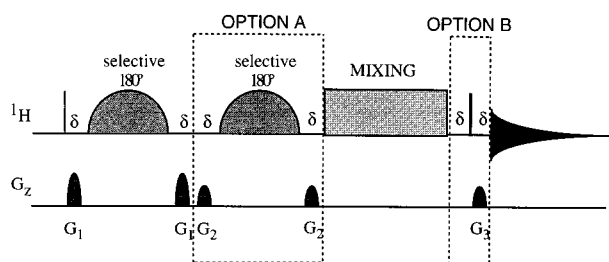
Figure 19. General scheme for recording gradient-based selective 1D homonuclear experiments. Option A selects SPFGE *vs.* DPFGE as a method of selective excitation. Option B selects for a refocusing gradient without the need for phase cycling or no refocusing gradient with a four-step EXORCYCLE cycle on a selective 180° pulse. See Table 1 for some homonuclear mixing processes.

sensitivity losses due to coherence selection and diffusion effects. In practice, the last alternative also gives the high-quality spectra and can be used as a general way to perform such experiments with maximum sensitivity.

Some examples of selective gradient-based 1D experiments have been described and clearly illustrated for the 1D COSY,[100,212,214,220,223,239] 1D multiple-step RELAY,[212,214,223] 1D TOCSY,[208-210,223,224] 1D ROESY,[208,209,224] 1D NOESY,[211,221,222,225] 1D COSY-NOESY,[213] 1D TOCSY-NOESY,[213,224] 1D TOCSY-ROESY[213] and 1D ROESY-TOCSY[213] experiments. Other combined experiments are also reliable. Recently, analogous experiments using PFGs for coherence rejection have also been shown to afford high-quality spectra without the sensitivity losses associated with conventional coherence selection. Usually these PFGs are placed in the mixing time of NOESY experiments or flanking the DIPSI scheme in z-filtered TOCSY experiments. Applications of selective 1D TOCSY, NOESY, TOCSY-TOCSY, NOESY-NOESY, TOCSY-NOESY and NOESY-TOCSY have been illustrated using oligo- and polysaccharide samples.[240] Finally, a particular case of selective 1D experiments has been proposed to study solvent–solute interactions.[41,204,207,212,241-249] The initial starting
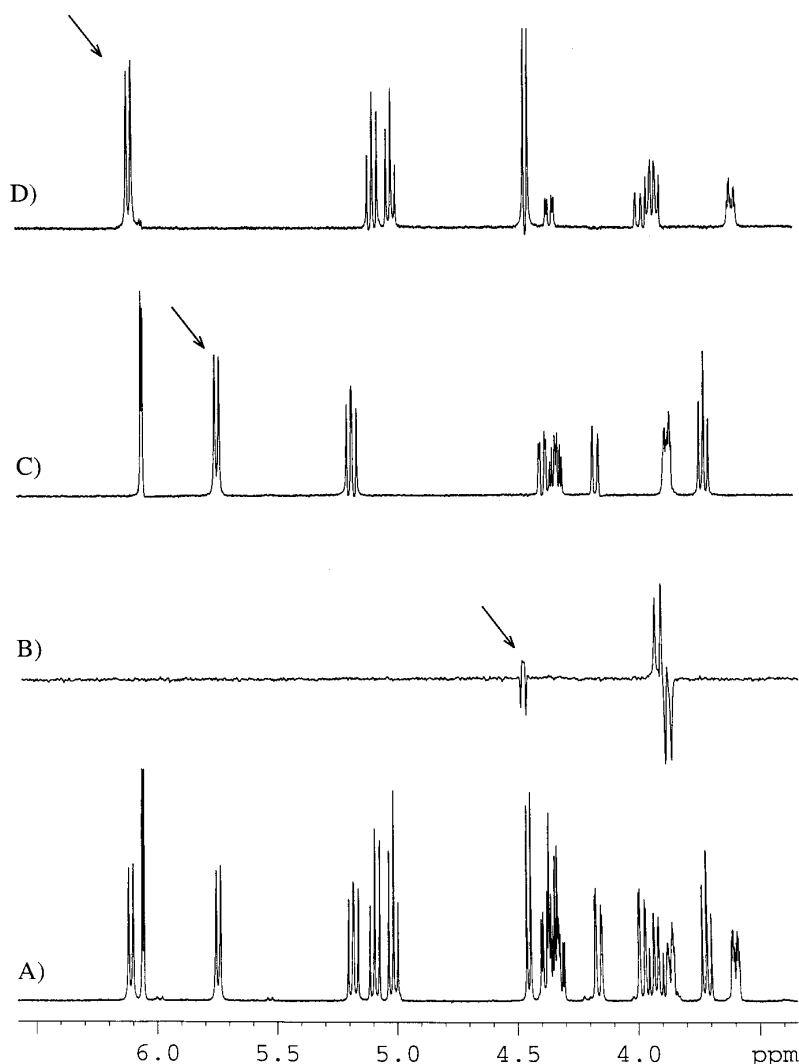

Figure 20. Selective 1D (B) DPFGE-COSY and (C) and (D) DPFGE-TOCSY spectra of chentobiose in CDCl₃; eight scans were recorded for each spectrum. Arrows indicate where the selective 180° pulses is applied. In (B) a defocusing *J* delay of 40 ms was used. The mixing times in (C) and (D) were 80 ms using a 7.4. kHz MLEV-17 pulse train.
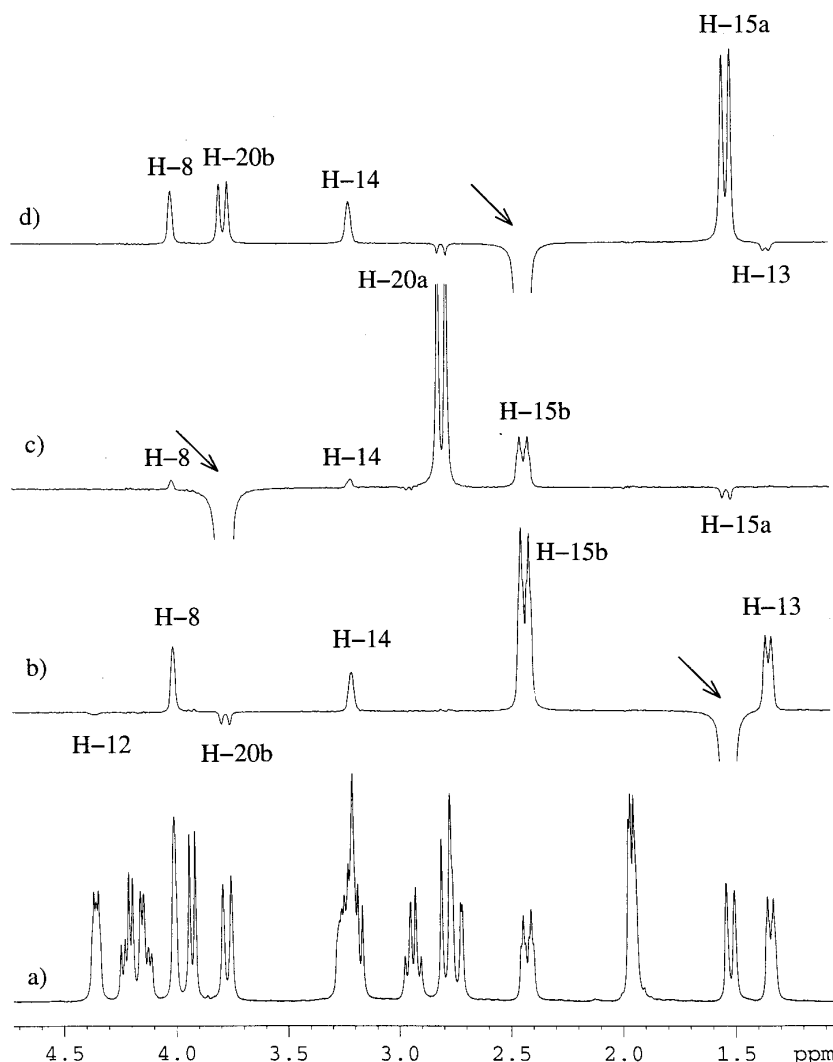
Figure 21. Some selective 1D DPFGE-NOESY spectra of strychnine with a mixing time of 900 ms. The selective 180° pulse was of 40 ms duration with a Gaussian shape truncated to 5%. Four gradients of 1 ms of duration were applied in the DPFGE block with intensities of 3, 3, 7 and 7 G cm^{-1}. A purge gradient of 1 ms duration and 6 G cm^{-1} intensity was applied during the mixing time.

point for these selective 1D EXSY experiments is the selective excitation of the water signal and the further observation of chemical exchange and dipolar interactions between water and protons belonging to biomolecules.

As examples, Fig. 20 shows some high-quality 1D DPFGE-COSY and DPFGE-TOCSY spectra quickly recorded for the peracetylated disaccharide chentobiose. Figure 21 shows some 1D DPFGE-NOESY spectra on strychnine. In this case, the ultra-clean spectra allow the identification of very small NOEs and even indirect NOEs. A recent extensive and very comprehensive study analyzing spin dynamics of gradient-enhanced 1D NOE experiments has been published and modifications to eliminate undesired SPT effects have been proposed.[225]

From this general methodology, it is possible to design 2D analog by concatenating other homonuclear 2D building blocks to the mentioned 1D experiments. For instance, Fig. 22 shows the basic pulse sequences to record 2D selective-TOCSY-COSY and 2D selective-TOCSY-J-resolved experiments. Figure 23 shows as an example the ultra-clean 2D COSY subspectra of each residue of chentobiose acquired under the same experimental conditions as in Fig. 20(C) and (D).

It is also possible to design heteronuclear selective 1D experiments using the basic gradient-enhanced HMQC and HSQC pulse trains. Applications have been described for proton-detected 1D HMQC and 1D HSQC,[200,250–253] 1D HMBC,[250–252] 1D HMQC-TOCSY,[250,251] 1D HSQC-TOCSY,[251,254,255] HET-GOESY,[226] 1D HSQC-NOESY,[162b,251] X-INEPT,[256] 1D HSQC-ROESY,[251] 1D HMQC-NOESY,[251] 1D HMQC-ROESY,[251] 1D HMQC-COSY,[251] 1D HSQC-COSY,[251] 1D HMQC-RELAY,[251] and 1D HSQC-RELAY[251] experiments. PEP methodology can be also incorporated in selective 1D HMQC, HSQC, X-INEPT[200] (Fig. 15) and HSQC-TOCSY experiments,[257] achieving a sensitivity enhancement of a factor of 2 for IS systems. On the other hand, some
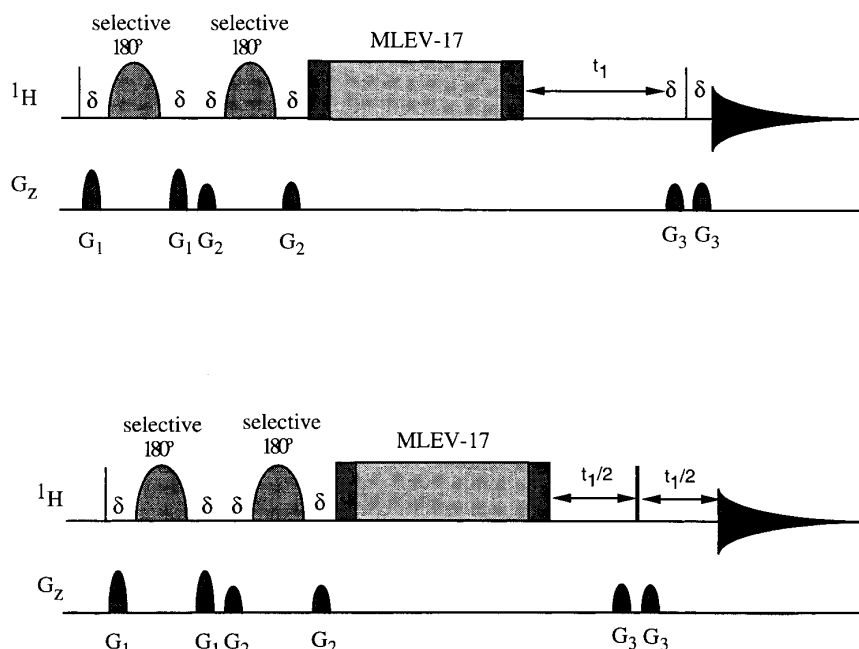
Figure 22. Concatenation of selective 1D experiments with classical 2D schemes: pulse sequences for recording gradient-based 2D selective-TOCSY-COSY and 2D selective-TOCSY-J-resolved experiments. A four-step EXORCYCLE phase cycling is applied on the first selective 180° pulse and the receiver. Gradients must be optimized in order to avoid unwanted refocusing.

selective carbon-detected heteronuclear 1D experiments have been also proposed, such as the selective 1D INADEQUATE[100] and GRECCO[258] experiments.

Semi-selective excitation

A serious drawback of multi-dimensional spectra is their low resolution. Sometimes, the analysis of a specific region which has many overlapping resonances can be of interest. For this reason, some nD experiments using semi-selective excitation have been proposed.[214–217,227,231–233,259,260] The simplest way to convert a gradient-based 2D experiment into an analogous semi-selective experiment is to replace the hard 180° pulse incorporated in the spin-echo period by a semi-selective 180° pulse [Fig. 24(a)]. In this case, PFGs must be applied before and after this pulse as described for the SPFGE block. Semi-selective excitation can be applied for both the F_1 and F_2 dimensions. However, in modern spectrometers equipped with digital filters, automatic selection on the F_2 dimension can be accomplished without the need to modify the original sequence. Figure 24(b) is a general scheme to acquire homonuclear F_1-semi-selective 2D experiments using the echo–antiecho approach.

As an example, a simple way to acquire the fingerprint COSY region of a protein in H_2O without presaturation and with improved resolution is to replace the excitation and mixing 90° pulses of the conventional COSY pulse sequence by two SPFGE blocks.[216] Figure 25(c) shows the H_α–NH region of a phase-sensitive

COSY obtained with this approach. Another advantage to use semi-selective excitation is the absence of diagonal peaks in the F_2 spectral region of interest and, therefore, the spectra contain significantly less t_1 noise.

In modern spectrometers, the combination of digital filtering, oversampling and PFG affords a powerful way to obtain improved sensitivity and resolution in multi-dimensional experiments without the presence of undesired folded peaks and without the need to modify standard sequences. Figure 26 compares expanded regions obtained from (A) a full 2D DQF-COSY spectrum acquired without digital filtering, (B) the aliphatic region of a 2D DQF-COSY with digital filtering and (C) phase-sensitive 2D DQF-COSY with digital filtering of a sample of progesterone. The experimental conditions are the same for all spectra. In Fig. 27 we show the same feature obtained from a 2D HMBC spectra of chentobiose (A) without and (B) with digital filtering.

Solvent suppression

In principle, gradient-based experiments achieve frequency-independent solvent suppression by using the inherent dephasing effects of PFGs. However, the signal arising from H_2O is very intense, and the use of additional specific schemes is required to improve the suppression.[261] The most accepted approach is the WATERGATE scheme,[127,128] which uses the same principles as discussed above for the SPFGE. Figure 28 shows the general scheme to record homonuclear 2D
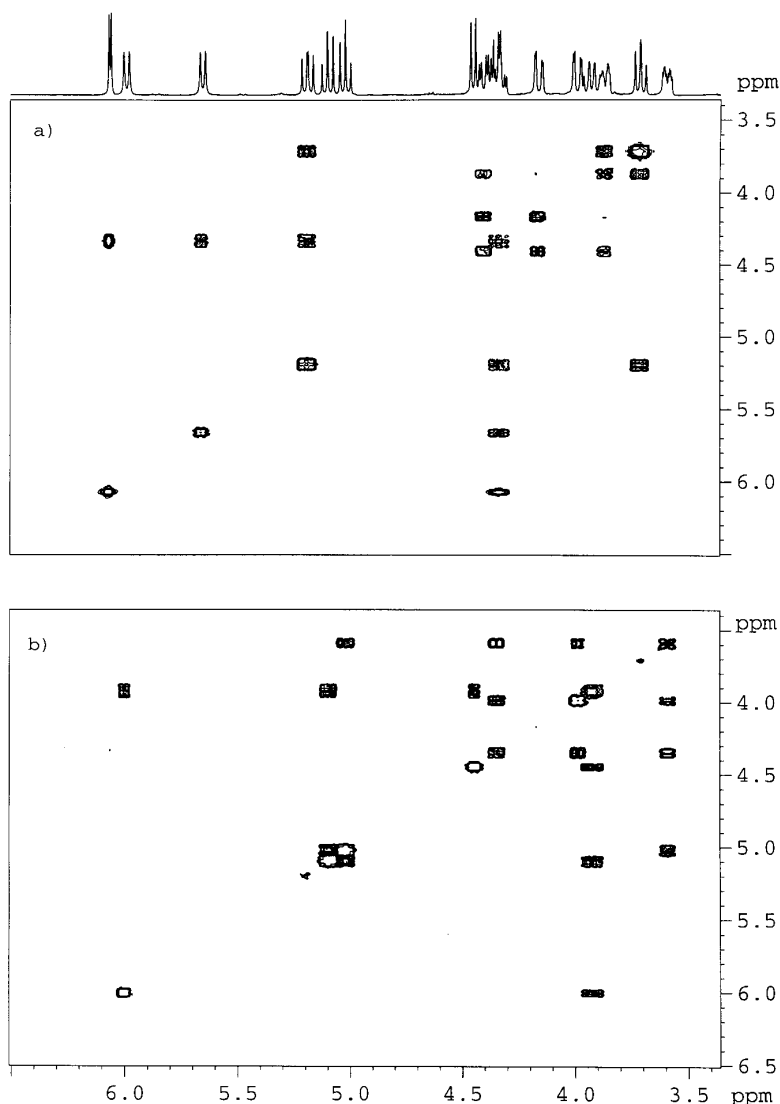
Figure 23. 2D selective-TOCSY-COSY subspectra of the two residues of chentobiose recorded with the pulse sequence of Fig. 22 (top). The duration of G_1, G_2 and G_3 was 1 ms and their strength were set to 5, 3.5 and 4 G cm^{-1}, respectively. Four transients for each 256 t_1 increments were acquired. All other experimental details as described in Fig. 20(C) and (D), respectively.

experiment using WATERGATE. On the other hand, the WATERGATE with water flip-back approach has also been proposed to restore water magnetization to its equilibrium state. Several applications have been given, such in 2D TOCSY,[262,263] 2D NOESY,[264–266] 2D ROESY[267a] and 2D HSQC[128] experiments.

Analogous solvent suppression using the DPFGE scheme has been proposed[219] and extended to 2D applications,[220] although transverse relaxation and the evolution of couplings can be troublesome. A closely related experiment, named MEGA,[267] combines the excellent tolerance to imperfections of the DPFGE scheme and the short echo times of the WATERGATE approach.

As an alternative to these echo-based schemes, the suppression of the undesired solvent signal can be performed with the CHESS sequence,[268] which consists in the frequency-selective excitation of the water followed

by a dephasing PFG. A similar approach, the RAW experiment, has proved to be very useful as a preparation period in homonuclear 2D experiments.[78] Improved suppression is achieved with the more sophisticated WET scheme, which uses a series of variable flip-angle solvent-selective r.f. pulses, where each selective r.f. pulse is followed by a dephasing gradient.[77,269] This scheme is very useful for LC–NMR (for multiple-solvent suppression) and high-resolution NMR applications such as DQF-COSY, TOCSY, NOESY and inverse experiments. Multiple-solvent suppression can also be achieved using magic-angle gradients in DQ experiments[94] or using modified SPFGE[214] and DPFGE schemes.[229,230]

Other useful methods using PFGs to suppress the intense solvent signal in biological samples includes the Water-PRESS[270,271] and the DRYCLEAN[272] approaches, which take advantage of the different relax-
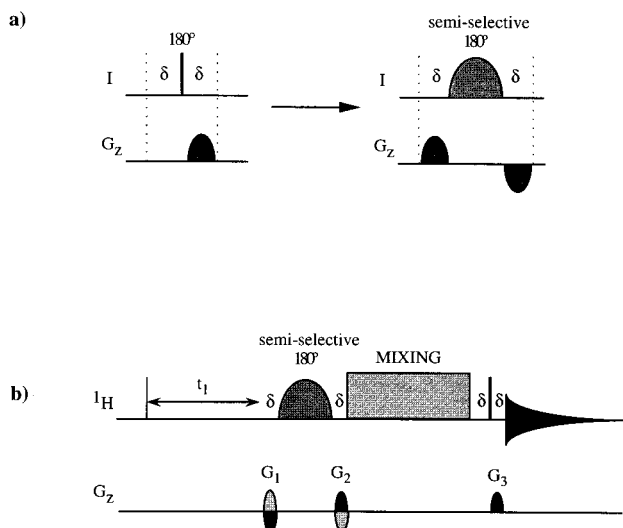
Figure 24. (a) Simple building block derived from a conventional gradient echo to achieve semi-selective excitation in the F_1 dimension and (b) general scheme to record w_1-selective 2D homonuclear experiments using an SPFGE scheme. See Table 1 for some possible mixing processes. As discussed in the text, the last G_3 gradient can be omitted at expense of an extended phase cycling.

ation and diffusion properties of the solvent and the biomolecules.

DIFFUSION ORDERED SPECTROSCOPY

Molecular diffusion studies can also be carried out using PFG-based NMR experiments.[1-3] The pioneering experiment to measure self-diffusion coefficients was the PFG-echo experiment.[273] Recently, improved methodologies to analyze biofluids and complex chemical mixtures by means of a new approach called diffusion ordered spectroscopy (DOSY)[274-277] have emerged. The basic 2D DOSY spectrum displays conventional chemical shifts in one dimension and diffusion rates in the other dimension. Because of the relationship between diffusion rates and molecular radii, the diffusion dimension reveals the distribution of molecular sizes and allows different molecular species to be identified and assigned. This diffusion dimension is achieved by recording consecutive spectra in which the gradient strengths are incremented.

Resolution in the diffusion dimension has been improved by removing eddy current effects by using bipolar gradients,[45] removing convection artefacts,[278] using high fields[279] and using 3D analogs of the basic 2D DOSY experiment: NOESY,[280] COSY,[281] TOCSY,[282-285] DQ[286] and heteronuclear-DOSY[287] experiments. The effects of chemical exchange and the measurement of exchange rates have been also discussed.[288] Related applications to measure molecular weight distributions,[289] to determine the molecular aggregation state[290-294] and protein unfolding[295] have also been described. Some applications to organic

supramolecular chemistry have also been described.[296-299]

A related approach based on the electrophoretic mobilities of contributing ions has been published.[300,301]

Editing of proton NMR spectra for biological fluids based on differences in molecular diffusion coefficients alone and the combination of relaxation and diffusion parameters has been presented.[302] These methods are also applicable to multi-dimensional homonuclear experiments, as demonstrated for 2D TOCSY experiments.

Alternative methods for measuring self-diffusion coefficients rely on r.f. gradients in place of the static PFG.[303-305]

RADIOFREQUENCY (B_1) GRADIENTS

As an alternative to coherence selection by B_0 gradients, a series of studies have dealt with the possibility of performing this selection by using radiofrequency (B_1) gradients. Some advantages of such approaches are as follows: (i) no need for recovery times after the gradient and, therefore, eddy current effects are avoided; (ii) no need for pre-emphasis; (c) the lineshape is not distorted; (iii) the gradient is frequency selective; (iv) the lock system is not perturbed; and (v) the B_1 gradient pulse acts simultaneously for excitation and for defocusing–refocusing purposes. Theoretical and practical aspects of B_1 gradients have recently been reviewed.[306-308] Applications to solvent suppression,[309,310] 2D COSY,[311,312] 2D NOESY,[313,314] 2D COSY-DQF,[315,316] 2D HSQC,[317] selective 1D COSY,[318] isotope filtering[237,319] and molecular diffusion[303-305] experiments have been described. A DPFGE scheme using r.f. gradients has been theoretically analyzed and compared with the original sequence.[216]

CONCLUSIONS

The incorporation of PFGs in pulse sequences has became indispensable in running the most modern and useful NMR experiments under the most optimum conditions. Compared with conventional analogous phase-cycled experiments, improved spectral quality is usually achieved in shorter acquisition times. Such advantages combined with the powerful available software packages offer to chemists a powerful tool to obtain valuable information about chemical structures and dynamics in a simple way.

Acknowledgements
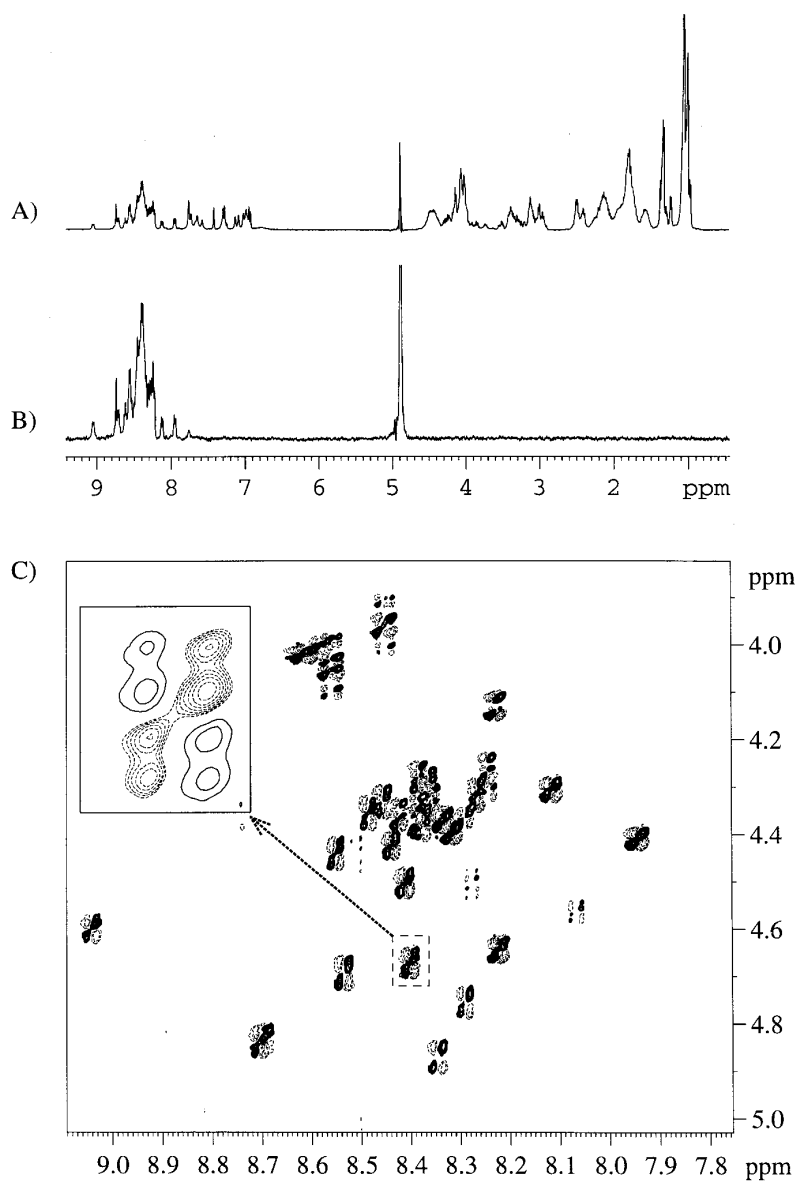
Figure 25. (A)^{1}H 400 MHz spectrum of salmon calcitonin in 90% H_2O–10% D_2O after applying the WATERGATE scheme; (B) semi-selective excitation of the NH proton region using an SPFGE scheme and without applying any solvent suppression scheme; (C) the fingerprint region of the w_1, w_2-semi-selective 2D COSY spectrum using the pulse sequence described in Ref. 216. The SPFGE block consists of an RE-BURP pulse of 11 ms applied as a shaped-DANTE pulse train.[259] In the inset, note the excellent resolution in the w_1 dimension for a given cross peak.

A) B) C)

Figure 26. Experimental effect of applying digital filtering on gradient-based DQF-COSY spectra of progesterone (A)–(C) are expansions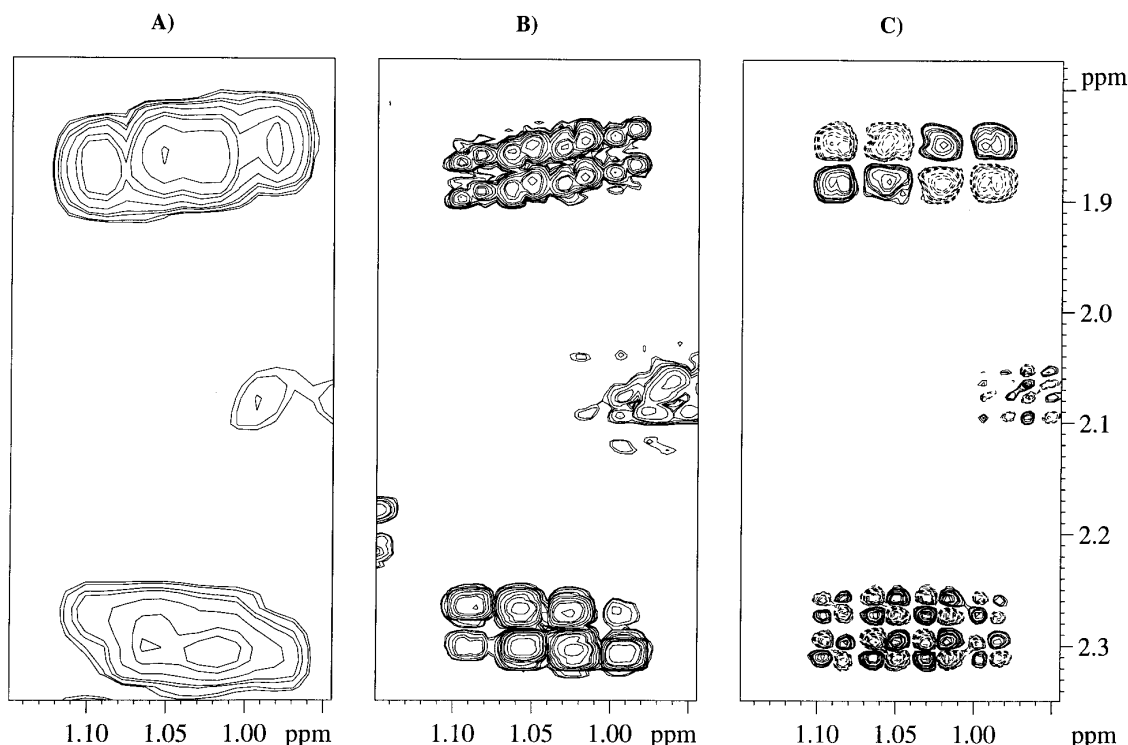 of (A) a magnitude-mode spectrum recorded with a spectral width of 5.82 ppm in both dimensions [see Fig. 4b]; (B) as (A) but using a spectral width of 1.90 ppm in both dimensions; and (C) phase-sensitive spectrum recorded as (B) using the scheme in Fig. 4(c).
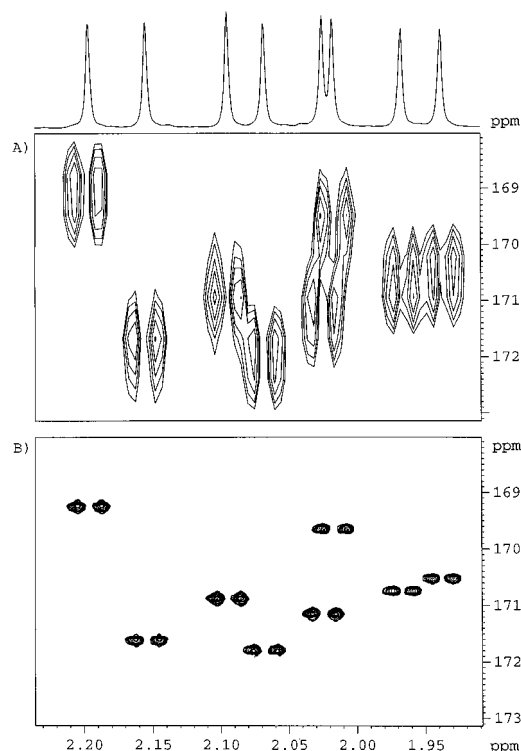

Figure 27. Experimental effect of applying digital filtering on gradient-based ^1H–^{13}C HMBC spectra of chentobiose (defocusing delay Δ_2 of 60 ms) using the pulse sequence sketched in Fig. 9a: (A) Expansion plot of the carbonyl region acquired with $SW(F_2) = 5.70$ ppm and $SW(F_1) = 160$ ppm; (B) as (A) but $SW(F_2) = 0.7$ ppm and $SW(F_1) = 11$ ppm. No folded peaks in the F_1 dimension were observed.
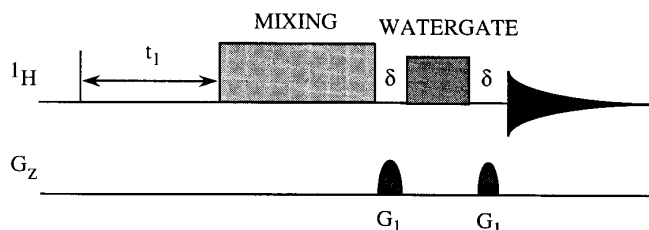

Figure 28. General scheme for recording 2D homonuclear experiments using the WATERGATE scheme. See Table 1 for homonuclear mixing processes.

REFERENCES

1. P. Stilbs, *Prog. Nucl. Magn. Reson. Spectrosc.* **19**, 1 (1987).
2. W. S. Price, *Annu. Rep. NMR Spectrosc.* 51 (1996).
3. C. S. Johnson, Jr, in *Encyclopedia of NMR*, edited by R. K. Harris and D. M. Grant, Vol. 3, p. 1626. Wiley, Chichester (1996).
4. W. E. Maas, F. H. Laukien and D. G. Cory, *J. Am. Chem. Soc.* **118**, 13085 (1996).
5. J. C. Lindon, J. K. Nicholson and I. D. Wilson, *Prog. Nucl. Magn. Reson. Spectrosc.* **29**, 1 (1996).
6. G. Bodenhausen, H. Kogler and R. R. Ernst, *J. Magn. Reson.* **58**, 370 (1984).
7. R. R. Ernst, G. Bodenhausen and A. Wokaun, in *Principles of Nuclear Magnetic Resonance in One and Two Dimensions.* Oxford University Press, Oxford (1987).
8. A. A. Maudsley, A. Wokaun and R. R. Ernst, *Chem. Phys. Lett.* **55**, 9 (1978).
9. A. Bax, P. G. de Jong, A. F. Mehlkopf and J. Smidt, *Chem. Phys. Lett.* **69**, 567 (1980).
10. P. Barker and R. Freeman, *J. Magn. Reson.* **64**, 334 (1985).
11. J. Keeler, R. T. Clowes, A. L. Davies and E. D. Laue, *Methods Enzymol.* **239**, 145 (1994).

12. T. Parella, *Magn. Reson. Chem.* **34**, 329 (1996).
13. S. Berger, *Prog. Nucl. Magn. Reson. Spectrom.* **30**, 137 (1997).
14. T. Norwood, *Chem. Soc. Rev.* **23**, 59 (1994).
15. J. M. Zhu and I. C. P. Smith, *Concepts Magn. Reson.* **7**, 281 (1995).
16. J. R. Tolman and J. H. Prestegard, *Concepts Magn. Reson.* **7**, 247 (1995).
17. L. E. Kay, *Curr. Opin. Struct. Biol.* **5**, 674 (1995).
18. D. M. Doddrell, *J. Chin. Chem. Soc.* **38**, 107 (1991).
19. R. E. Hurd, in *Encyclopedia of NMR*, edited by R. K. Harris and D. M. Grant, Vol. 3, p. 1990. Wiley, Chichester (1996).
20. S. Braun, H.-O. Kalinowski and S. Berger, *100 and More Basic NMR Experiments*. VCH, Weinheim (1996).
21. A. L. Davis, R. Boelens and R. Kaptein, *J. Biomol. NMR* **2**, 395 (1992).
22. I. M. Brereton, S. Crozier, J. Field and D. M. Doddrell, *J. Magn. Reson.* **93**, 54 (1991).
23. M. von Kienlin, C. T. W. Moonen, A. van der Toorn and P. C. M. van Zijl, *J. Magn. Reson.* **93**, 423 (1991).
24. A. L. Davis, J. Keeler, E. D. Laue and D. Moskau, *J. Magn. Reson.* **98**, 207 (1992).
25. D. J. States, R. A. Haberkorn and D. J. Ruben, *J. Magn. Reson.* **48**, 286 (1982).
26. J. Cavanagh, A. G. Palmer, III, P. E. Wright and M. Rance, *J. Magn. Reson.* **91**, 429 (1991).
27. A. G. Palmer, III, J. Cavanagh, P. E. Wright and M. Rance, *J. Magn. Reson.* **93**, 151 (1991).
28. J. Cavanagh and M. Rance, in *Annu. Rep. NMR Spectrosc.* **27**, 1 (1993).
29. M. Sattler, M. G. Schwendinger, J. Schleucher and C. Griesinger, *J. Biomol. NMR* **6**, 11 (1995).
30. M. Sattler, P. Schmidt, J. Schleucher, O. Schedletzky, S. J. Glaser and C. Griesinger, *J. Magn. Reson. B* **108**, 235 (1995).
31. S. S. Wijmenga, C. P. M. van Mierlo and E. Steensma, *J. Biomol. NMR* **8**, 319 (1996).
32. R. E. Hurd, B. K. John and D. Plant, *J. Magn. Reson.* **93**, 666 (1991).
33. A. Bax and S. S. Pochapsky, *J. Magn. Reson.* **99**, 638 (1992).
34. P. C. M. Van Zijl, S. Sukumar, M. O. Johnson, P. Webb and R. E. Hurd, *J. Magn. Reson. A* **111**, 203 (1994).
35. S. Sukumar, M. O. Johnson, R. E. Hurd and P. C. M. van Zijl, *J. Magn. Reson.* **125**, 159 (1997).
36. R. E. Hurd, A. Deese, M. O. Johnson, S. Sukumar and P. C. M. van Zijl, *J. Magn. Reson. A* **119**, 285 (1996).
37. M. Czisch, A. Ross, C. Cieslar and T. A. Holak, *J. Biomol. NMR* **7**, 121 (1996).
38. P. B. Kingsley, *J. Magn. Reson. B* **109**, 243 (1995).
39. S. Zhang and D. G. Gorenstein, *J. Magn. Reson. A* **118**, 291 (1996).
40. V. Sklenár, *J. Magn. Reson. A* **114**, 132 (1995).
41. A. Böckmann and E. Guittet, *J. Biomol. NMR* **8**, 87 (1996).
42. G. Wider, V. Dotsch and K. Wüthrich, *J. Magn. Reson. A* **108**, 255 (1994).
43. V. Dötsch, G. Wider and K. Wüthrich, *J. Magn. Reson. A* **109**, 263 (1994).
44. V. Dötsch and G. Wider, *J. Am. Chem. Soc.* **117**, 6064 (1995).
45. D. Wu, A. Chen and C. S. Johnson, Jr, *J. Magn. Reson. A* **115**, 260 (1995).
46. A. L. Davis, G. Escourt, J. Keeler, E. D. Laue and J. J. Titman, *J. Magn. Reson. A* **105**, 167 (1993).
47. M. Czisch, G. C. King and A. Ross, *J. Magn. Reson.* **126**, 154 (1997).
48. K. Zangger and H. Sterk, *J. Magn. Reson.* **124**, 486 (1997).
49. T. A. Carpenter, L. D. Colebrook, L. D. Hall and G. K. Pierens, *Magn. Reson. Chem.* **30**, 768 (1992).
50. T. Parella, unpublished work.
51. R. E. Hurd, *J. Magn. Reson.* **87**, 422 (1990).
52. A. Otter and D. R. Bundle, *J. Magn. Reson. B* **109**, 194 (1995).
53. T. J. Horne and G. A. Morris, *J. Magn. Reson. A* **123**, 246 (1996).
54. T. J. Horne and G. A. Morris, *Magn. Reson. Chem.* **35**, 680 (1997).
55. M. A. McCoy and W. S. Warren, *J. Chem. Phys.* **93**, 858 (1990).
56. W. S. Warren, Q. He, M. McCoy and F. C. Spano, *J. Chem. Phys.* **96**, 1659 (1992).
57. W. S. Warren, W. Richter, A. H. Andreotti and B. T. Farmer, II, *Science* **262**, 2005 (1993).
58. Q. He, W. Richter, S. Vathyam and W. S. Warren, *J. Chem. Phys.* **98**, 6779 (1993).
59. P. R. Bachiller, S. Ahn and W. S. Warren, *J. Magn. Reson. A* **122**, 94 (1996).
60. J. Jeener, A. Vlassenbroek and P. Broekaert, *J. Chem. Phys.* **103**, 1309 (1995).
61. S. Lee, W. Richter, S. Vathyam and W. S. Warren, *J. Chem. Phys.* **105**, 874 (1996).
62. S. Vathyam, S. Lee and W. S. Warren, *Science* **267**, 654 (1995).
63. W. Richter, S. Lee, W. S. Warren and Q. He, *Science* **272**, 92 (1996).
64. W. S. Warren, S. Lee, W. Richter and S. Vathyam, *Chem. Phys. Lett.* **247**, 207 (1995).
65. G. J. Bowden, T. Heseltine and M. J. Prandolini, *Chem. Phys. Lett.* **233**, 639 (1995).
66. W. S. Warren and W. Richter, in *Encyclopedia of NMR*, edited by R. K. Harris and D. M. Grant, Vol. 3, p. 1417. Wiley, Chichester (1996).
67. M. H. Levitt, *Concepts Magn. Reson.* **8**, 77 (1996).
68. S. Ahn, W. S. Warren and S. Lee, *J. Magn. Reson.* **128**, 114 (1997).
69. A. L. Davis, E. D. Laue, J. Keeler, D. Moskau and J. Lohman, *J. Magn. Reson.* **94**, 637 (1991).
70. A. A. Shaw, C. Salaun, J.-F. Dauphin and B. Ancian, *J. Magn. Reson. A* **120**, 110 (1996).
71. B. Ancian, I. Bourgeois, J.-F. Dauphin and A. A. Shaw, *J. Magn. Reson.* **125**, 348 (1997).
72. W. Willker, D. Leibfritz, R. Kerssebaum and J. Lohman, *J. Magn. Reson. A* **102**, 348 (1993).
73. B. K. John, D. Plant, P. Webb and R. E. Hurd, *J. Magn. Reson.* **99**, 200 (1992).
74. L. A. Trimble and M. A. Bernstein, *J. Magn. Reson. B* **105**, 67 (1994).
75. P. C. M. van Zijl, M. O. Johnson, S. Mori and R. E. Hurd, *J. Magn. Reson. A* **113**, 265 (1995).
76. D. L. Mattiello, W. S. Warren, L. Muller and B. T. Farmer, II, *J. Am. Chem. Soc.* **118**, 3253 (1996).
77. S. H. Smallcombe, S. L. Patt and P. A. Keifer, *J. Magn. Reson. A* **117**, 295 (1995).
78. A. S. Altieri and R. A. Byrd, *J. Magn. Reson. B* **107**, 260 (1995).
79. T. Parella, F. Sánchez-Ferrando and A. Virgili, *J. Magn. Reson.* **125**, 145 (1997).
80. R. Wagner and S. Berger, *J. Magn. Reson. A* **123**, 119 (1996).
81. M. Baur and H. Kessler, *Magn. Reson. Chem.* **35**, 877 (1997).
82. C. T. W. Moonen, P. van Gelderen, G. W. Vuister and P. C. M. van Zijl, *J. Magn. Reson.* **97**, 419 (1992).
83. D. Abergel, A. Louis-Joseph and J.-Y. Lallemand, *J. Biomol. NMR* **8**, 15 (1996).
84. C. H. Sotak, D. M. Freeman and R. E. Hurd, *J. Magn. Reson.* **78**, 355 (1988).
85. A. Wilman and P. S. Allen, *J. Magn. Reson. B* **101**, 165 (1993).
86. A. Wilman and P. S. Allen, *J. Magn. Reson. B* **105**, 58 (1994).
87. A. Wilman and P. S. Allen, *J. Magn. Reson. B* **109**, 169 (1995).
88. J. E. van Dijk, A. F. Mehlkopf and W. M. M. J. Bovée, *NMR Biomed.* **5**, 75 (1992).
89. G. A. Naganagowda, *J. Magn. Reson. A* **113**, 235 (1995).
90. G. A. Naganagowda, *J. Magn. Reson. A* **118**, 113 (1996).
91. G. K. Pierens, T. A. Carpenter, L. D. Colebrook, L. D. Field and L. D. Hall, *J. Magn. Reson.* **99**, 398 (1992).
92. C. Dalvit and J. M. Böhlen, *J. Magn. Reson. B* **111**, 76 (1996).
93. C. Dalvit and J. M. Böhlen, *J. Magn. Reson. B* **113**, 195 (1996).
94. C. Dalvit and J. M. Böhlen, *Magn. Reson. Chem.* **34**, 829 (1996).
95. C. Dalvit, *J. Magn. Reson. B* **110**, 225 (1996).
96. C. Dalvit, *J. Magn. Reson. B* **112**, 186 (1996).
97. C. Dalvit and J. M. Böhlen, *J. Magn. Reson.* **126**, 149 (1997).
98. J. Balbach and H. Kessler, *J. Magn. Reson. B* **105**, 83 (1994).
99. H. Desvaux, *J. Magn. Reson.* **127**, 1 (1997).
100. W. Willker and D. Leibfritz, *Magn. Reson. Chem.* **32**, 665 (1994).
101. N. C. Nielsen, H. Thogersen and O. W. Sorensen, *J. Chem. Phys.* **105**, 3962 (1996).
102. N. C. Nielsen, H. Thogersen and O. W. Sorensen, *J. Am. Chem. Soc.* **117**, 11365 (1995).
103. N. C. Nielsen and O. W. Sorensen, *J. Magn. Reson. A* **123**, 135 (1996).
104. A. Bax and S. Subramanian, *J. Magn. Reson.* **67**, 565 (1986).
105. B. A. Messerle, G. Wider, G. Otting, C. Weber and K. Wüthrich, *J. Magn. Reson.* **85**, 608 (1989).
106. R. E. Hurd and B. K. John, *J. Magn. Reson.* **91**, 648 (1991).
107. G. Kontaxis, J. Stonehouse, E. D. Laue and J. Keeler, *J. Magn. Reson.* **111**, 70 (1994).
108. J. A. Gavin, J. L. Pons and M. A. Delsuc, *J. Magn. Reson. A* **122**, 64 (1996).
109. J. Schleucher, M. G. Schwendinger, M. Sattler, P. Schmidt, O. Schedletzky, S. J. Glaser, O. W. Sorensen and C. Griesinger, *J.*

Biomol. NMR **4**, 301 (1994).
110. J. Schleucher, M. Sattler and C. Griesinger, *Angew. Chem., Int. Ed. Engl.* **32**, 1489 (1993).
111. M. Sattler, J. Schleucher, O. Schedletzky, S. J. Glaser, C. Griesinger, N. C. Nielsen and O. W. Sorensen, *J. Magn. Reson. A* **119**, 171 (1996).
112. G. W. Vuister, R. Boelens, R. Kaptein, R. E. Hurd, B. K. John and P. C. M. van Zijl, *J. Am. Chem. Soc.* **113**, 9688 (1991).
113. J. Ruiz-Cabello, G. W. Vuister, C. T. W. Moonen, P. V. Gelderen, J. S. Cohen and P. C. M. van Zijl, *J. Magn. Reson.* **100**, 282 (1992).
114. J. Boyd, N. Soffe, B. K. John, D. Plant and R. Hurd, *J. Magn. Reson.* **98**, 660 (1992).
115. L. E. Kay, P. Keifer and T. Saarinen, *J. Am. Chem. Soc.* **114**, 10663 (1992).
116. M. Sattler, M. Maurer, J. Schleucher and C. Griesinger, *J. Biomol. NMR* **5**, 97 (1995).
117. J. R. Tolman and J. H. Prestegard, *J. Magn. Reson. B* **112**, 245 (1996).
118. J. R. Tolman and J. H. Prestegard, *J. Magn. Reson. B* **112**, 269 (1996).
119. K. T. Dayie and G. Wagner, *J. Magn. Reson. A* **111**, 121 (1994).
120. Y. Li and G. Montelione, *J. Magn. Reson. B* **101**, 315 (1993).
121. F. A. A. Mulder, C. A. E. M. Spronk, M. Slijper, R. Kaptein and R. Boelens, *J. Biomol, NMR* **8**, 223 (1996).
122. W. Willker, D. Leibfritz, R. Kerssebaum and W. Bermel, *Magn. Reson. Chem.* **31**, 287 (1993).
123. T. Parella, unpublished work.
124. V. Dötsch, R. E. Oswald and G. Wagner, *J. Magn. Reson. B* **108**, 285 (1995).
125. B. K. John, D. Plant and R. E. Hurd, *J. Magn. Reson. A* **101**, 113 (1993).
126. G. Wider and K. Wüthrich, *J. Magn. Reson. B* **102**, 239 (1993).
127. M. Piotto, V. Saudek and V. Sklenár, *J. Biomol. NMR* **2**, 661 (1992).
128. V. Sklenár, M. Piotto, R. Leppik and V. Saudek, *J. Magn. Reson. A* **102**, 241 (1993).
129. S. Grzesiek and A. Bax, *J. Am. Chem. Soc.* **115**, 12593 (1993).
130. J. Stonehouse, G. L. Shaw, J. Keeler and E. D. Laue, *J. Magn. Reson. A* **107**, 178 (1994).
131. Y. Li and G. Montelione, *J. Magn. Reson. B* **105**, 45 (1994).
132. S. Mori, C. Abeygunawarda, M. O. Johnson and P. C. M. van Zijl, *J. Magn. Reson. B* **108**, 94 (1995).
133. P. C. M. van Zijl, T. L. Hwang, M. O. Johnson and M. Garwood, *J. Am. Chem. Soc.* **118**, 5510 (1996).
134. J. Stonehouse, R. T. Clowes, G. J. Shaw, J. Keeler and E. D. Laue, *J. Biomol. NMR* **5**, 226 (1995).
135. M. Tyburn, I. M. Brereton and D. M. Doddrell, *J. Magn. Reson.* **98**, 305 (1992).
136. J. R. Tolman, J. Chung and J. H. Prestegard, *J. Magn. Reson.* **98**, 462 (1992).
137. A. Ross, M. Czisch, C. Cieslar and T. A. Holak, *J. Biomol. NMR* **3**, 215 (1993).
138. G. W. Vuister, J. Ruiz-Cabello and P. C. M. van Zijl, *J. Magn. Reson.* **100**, 215 (1992).
139. P. C. M. van Zijl, M. O. Johnson and C. Abeygunawardana, *J. Magn. Reson. A* **108**, 116 (1994).
140. P. Bendel and P. C. M. van Zijl, *J. Magn. Reson. A* **110**, 130 (1994).
141. T. Parella, F. Sánchez-Ferrando and A. Virgili, *J. Magn. Reson.* **126**, 274 (1997).
142. T. Parella, J. Belloc, F. Sánchez-Ferrando and A. Virgili, in press (1998).
143. M. Liu, R. D. Farrant, J. K. Nicholson and J. C. Lindon, *J. Magn. Reson. A* **112**, 208 (1995).
144. M. Liu, J. K. Nicholson, J. C. Lindon, P. N. Sanderson and G. E. Tranter, *Magn. Reson. Chem.* **34**, 865 (1996).
145. M. Liu, R. D. Farrant, B. C. Sweatman, J. K. Nicholson and J. C. Lindon, *J. Magn. Reson. A* **113**, 251 (1995).
146. T. Parella, F. Sánchez-Ferrando and A. Virgili, *J. Magn. Reson. A* **117**, 78 (1995).
147. A. Bax, K. A. Farley and G. S. Walker, *J. Magn. Reson. A* **119**, 134 (1996).
148. W. Willker and D. Leibfritz, *Magn. Reson. Chem.* **33**, 632 (1995).
149. D. Uhrin, V. Varma and J. R. Brisson, *J. Magn. Reson. A* **119**, 120 (1996).
150. G. Zhu, D. Live and A. Bax, *J. Am. Chem. Soc.* **116**, 8370 (1994).
151. T. Parella, F. Sánchez-Ferrando and A. Virgili, *J. Magn. Reson. A* **112**, 241 (1995).
152. G. E. Martin, R. C. Crouch, M. H. M. Sharaf and P. L. Schiff, Jr,

J. Nat. Prod. **59**, 2 (1996).
153. S. Fukuzawa, S. Matsunaga and N. Fusetani, *Tetrahedron Lett.* **37**, 1447 (1996).
154. K. A. Farley, G. S. Walker and G. E. Martin, *Magn. Reson. Chem.* **35**, 671 (1997).
155. R. Malet, M. Moreno-Mañas, F. Pajuelo, T. Parella and R. Pleixats, *Magn. Reson. Chem.* **35**, 227 (1997).
156. J. C. Martins, F. Kayser, P. Verheyden, M. Gielen, R. Willem and M. Biesemans, *J. Magn. Reson.* **124**, 218 (1997).
157. R. Willem, A. Bouhdid, F. Kayser, A. Delmotte, M. Gielen, J. C. Martins, M. Biesemans, B. Mahieu and E. R. T. Tiekink, *Organometallics* **15**, 1920 (1996).
158. M. A. Keniry, *Magn. Reson. Chem.* **34**, 33 (1996).
159. R. E. Hurd and B. K. John, *J. Magn. Reson.* **92**, 658 (1991).
160. B. K. John, D. Plant, S. L. Heald and R. E. Hurd, *J. Magn. Reson.* **94**, 664 (1991).
161. R. C. Crouch, A. O. Davis and G. E. Martin, *Magn. Reson. Chem.* **33**, 889 (1995).
162. (a) K. E. Kövér, V. J. Hruby and D. Uhrin, *J. Magn. Reson.* **129**, 125 (1997); (b) R. Wagner and S. Berger, *Magn. Reson. Chem.* **35**, 199 (1997).
163. A. Majumdar and E. R. P. Zuiderweg, *J. Magn. Reson. B* **102**, 242 (1993).
164. J. Lee, J. Fejzo and G. Wagner, *J. Magn. Reson. B* **102**, 322 (1993).
165. G. W. Vuister, R. Boelens, R. Kaptein, M. Burgering and P. C. M. van Zijl, *J. Biomol. NMR* **2**, 301 (1992).
166. R. Harris, T. J. Rutherford, M. J. Milton and S. W. Homans, *J. Biomol. NMR* **9**, 47 (1997).
167. W. Jahnke, M. Baur, G. Gemmecker and H. Kessler, *J. Magn. Reson. B* **106**, 86 (1993).
168. J. Weigelt and G. Otting, *J. Magn. Reson. A* **113**, 128 (1995).
169. J. Weigelt and G. Otting, *J. Magn. Reson. A* **116**, 133 (1995).
170. T. K. Pratum, *J. Magn. Reson. A* **117**, 132 (1995).
171. T. K. Pratum, *J. Magn. Reson. B* **113**, 76 (1996).
172. J. Chung, J. R. Tolman, K. P. Howard and J. H. Prestegard, *J. Magn. Reson. B* **102**, 137 (1993).
173. T. Saito and P. L. Rinaldi, *J. Magn. Reson. A* **118**, 136 (1996).
174. B. Reif, M. Köck, R. Kerssebaum, H. Kang, W. Fenical and C. Griesinger, *J. Magn. Reson. A* **118**, 282 (1996).
175. M. Köck, B. Reif, W. Fenical and C. Griesinger, *Tetrahedron Lett.* **37**, 363 (1996).
176. A. Meissner, D. Moskau, N. C. Nielsen and O. W. Sørensen, *J. Magn. Reson.* **124**, 245 (1997).
177. B. Reif, M. Köck, R. Kerssebaum, J. Schleucher and C. Griesinger, *J. Magn. Reson. B* **112**, 295 (1996).
178. W. Kozminski, D. Sperandio and D. Nanz, *Magn. Reson. Chem.* **34**, 311 (1996).
179. W. Kozminski and D. Nanz, *J. Magn. Reson. A* **122**, 245 (1996).
180. G. Otting, B. A. Messerle and L. P. Soler, *J. Am. Chem. Soc.* **118**, 5096 (1996).
181. T. Facke, R. Wagner and S. Berger, *Concepts Magn. Reson.* **6**, 293 (1994).
182. S. Berger, T. Facke and R. Wagner, *Magn. Reson. Chem.* **34**, 4 (1996).
183. S. Berger, T. Facke, M. Gielen, R. Willem and B. Wrackmeyer (Eds), *Advanced Applications of NMR to Organometallic Chemistry*, Chapt. 2, pp. 29–44. John Wiley, New York (1996).
184. R. Wagner and S. Berger, *J. Magn. Reson. A* **120**, 258 (1996).
185. For a review, see G. Varani, F. Aboul-ela and F. H. T. Allain, *Prog. Nucl. Magn. Reson. Spectrosc.* **29**, 51 (1996).
186. C. Bauer, *Magn. Reson. Chem.* **34**, 532 (1996).
187. M. Liu, R. D. Farrant, J. M. Gillam, J. K. Nicholson and J. C. Lindon, *J. Magn. Reson. B* **109**, 275 (1995).
188. W. Kozminski and D. Nanz, *J. Magn. Reson.* **124**, 383 (1997).
189. W. Kozminski, S. Bienz, S. Bratovanov and D. Nanz, *J. Magn. Reson.* **125**, 193 (1997).
190. S. Bratovanov, W. Kozmisnki, J. Fassler, Z. Molnar, D. Nanz and S. Bienz, *Organometallics* **16**, 3128 (1997).
191. A. Meissner, J. Ø. Duus and O. W. Sørensen, *J. Magn. Reson.* **128**, 92 (1997).
192. M. D. Sørensen, J. Ø. Duus and O. W. Sørensen, *J. Biomol. NMR* **10**, 181 (1997).
193. A. Meissner, J. Ø. Duus and O. W. Sørensen, *J. Biomol. NMR* **10**, 89 (1997).
194. K. Ogura, H. Terasawa and F. Inagaki, *J. Biomol. NMR* **8**, 492 (1996).
195. G. Lippens, J.-M. Wieruszeski, P. Talaga and J.-P. Bohin, *J. Biomol. NMR* **8**, 311 (1996).
196. C. Zwahlen, P. Legault, S. J. F. Vincent, J. Greenblatt, R. Konrat

and L. E. Kay, *J. Am. Chem. Soc.* **119**, 6711 (1997).

197. D. Freeman, N. Sailasuta, S. Sukumar and R. E. Hurd, *J. Magn. Reson. B* **102**, 183 (1993).
198. R. A. Brown, R. A. Venters, P. P. Z. Tang and L. D. Spicer, *J. Magn. Reson. A* **113**, 117 (1995).
199. T. Parella and J. Belloc, unpublished work.
200. T. Parella, F. Sánchez-Ferrando and A. Virgili, *J. Magn. Reson.* **126**, 278 (1997).
201. J. Stelten and D. Leibfritz, *Magn. Reson. Chem.* **34**, 951 (1996).
202. T. Parella, F. Sánchez-Ferrando and A. Virgili, *J. Magn. Reson. B* **109**, 88 (1995).
203. M. Liu, R. D. Farrant, J. K. Nicholson and J. C. Lindon, *J. Magn. Reson. B* **106**, 270 (1995).
204. C. Dalvit and U. Hommel, *J. Magn. Reson. B* **109**, 334 (1995).
205. C. Dalvit and U. Hommel, *J. Biomol. NMR* **5**, 306 (1995).
206. C. Dalvit, *J. Magn. Reson. B* **112**, 282 (1996).
207. N. Birlirakis, R. Cerdan and E. Guittet, *J. Biomol. NMR* **8**, 487 (1996).
208. P. Adell, T. Parella, F. Sánchez-Ferrando and A. Virgili, *J. Magn. Reson. B* **108**, 77 (1995).
209. C. Dalvit and G. Bovermann, *Magn. Reson. Chem.* **33**, 156 (1995).
210. T. Fäcke and S. Berger, *J. Magn. Reson. A* **113**, 257 (1995).
211. J. Stonehouse, P. Adell, J. Keeler and A. J. Shaka, *J. Am. Chem. Soc.* **116**, 6037 (1994).
212. C. Dalvit, *J. Magn. Reson. A* **113**, 120 (1995).
213. P. Adell, T. Parella, F. Sánchez-Ferrando and A. Virgili, *J. Magn. Reson. A* **113**, 124 (1995).
214. C. Dalvit, S. Y. Ko and J. M. Böhlen, *J. Magn. Reson. B* **110**, 124 (1996).
215. C. Dalvit, *Magn. Reson. Chem.* **33**, 570 (1995).
216. C. Roumestand, P. Mutzenhardt, C. Delay and D. Canet, *Magn. Reson. Chem.* **34**, 807 (1996).
217. C. Le Guernevé and M. Seigneuret, *J. Biomol. NMR* **8**, 219 (1996).
218. V. Belle, G. Cros, H. Lahrech, P. Devoulon and M. Decorps, *J. Magn. Reson. A* **112**, 122 (1995).
219. T. L. Hwang and A. J. Shaka, *J. Magn. Reson. A* **112**, 275 (1995).
220. D. Callihan, J. West, S. Kumar, B. I. Schweitzer and T. M. Logan, *J. Magn. Reson. B* **112**, 82 (1996).
221. K. Stott, J. Stonehouse, J. Keeler, T. L. Hwang and A. J. Shaka, *J. Am. Chem. Soc.* **117**, 4199 (1995).
222. Q. N. Van and A. J. Shaka, *J. Magn. Reson. A* **119**, 295 (1996).
223. G. Xu and J. S. Evans, *J. Magn. Reson. B* **111**, 183 (1996).
224. M. J. Gradwell, H. Kogelberg and T. A. Frenkiel, *J. Magn. Reson.* **124**, 267 (1997).
225. K. Stott, J. Keeler, Q. N. Van and A. J. Shaka, *J. Magn. Reson.* **125**, 302 (1997).
226. K. Stott and J. Keeler, *Magn. Reson. Chem.* **34**, 554 (1996).
227. V. V. Krishnamurthy, *J. Magn. Reson. A* **121**, 33 (1996).
228. T. Parella, F. Sánchez-Ferrando and A. Virgili, *J. Magn. Reson.* in press (1998).
229. T. Parella, P. Adell, F. Sánchez-Ferrando and A. Virgili, *Magn. Reson. Chem.* **36**, 245 (1998).
230. C. Dalvit, *J. Biomol. NMR* submitted for publication.
231. V. V. Krishnamurthy, *J. Magn. Reson. B* **112**, 75 (1996).
232. V. V. Krishnamurthy, *J. Magn. Reson. B* **113**, 46 (1996).
233. V. V. Krishnamurthy, *Magn. Reson. Chem.* **35**, 9 (1997).
234. C. Emetarom, T. L. Hwang, G. Mackin and A. J. Shaka, *J. Magn. Reson. A* **113**, 137 (1995).
235. G. Mackin and A. J. Shaka, *J. Magn. Reson. A* **118**, 247 (1996).
236. G. Xu and J. S. Evans, *J. Magn. Reson. A* **123**, 105 (1996).
237. S. Heikkinen, E. Rahkamaa and I. Kilpeläinen, *J. Magn. Reson.* **127**, 80 (1997).
238. G. Bodenhausen, R. Freeman and D. L. Turner, *J. Magn. Reson.* **26**, 373 (1977).
239. M. A. Bernstein and L. A. Trimble, *Magn. Reson. Chem.* **32**, 107 (1994).
240. D. Uhrín and P. N. Barlow, *J. Magn. Reson.* **126**, 248 (1997).
241. V. Dotsch and G. Wider, *J. Am. Chem. Soc.* **117**, 6064 (1995).
242. R. W. Kriwacki, R. B. Hill, J. M. Flanagan, J. P. Caradonna and J. H. Prestegard, *J. Am. Chem. Soc.* **115**, 8907 (1993).
243. M. Andrec and J. H. Prestegard, *J. Biomol. NMR* **9**, 136 (1997).
244. S. Mori, M. O. Johnson, J. M. Berg and P. C. M. van Zijl, *J. Am. Chem. Soc.* **116**, 11982 (1994).
245. S. Mori, C. Abeygunawardana, P. C. M. van Zijl and J. M. Berg, *J. Magn. Reson. B* **110**, 96 (1996).
246. S. Mori, J. M. Berg and P. C. M. van Zijl, *J. Biomol. NMR* **7**, 77 (1996).
247. S. Mori, C. Abeygunawardana, J. M. Berg and P. C. M. van Zijl,

248. C. Sich, J. Flemming, R. Ramachandran and L. R. Brown, *J. Magn. Reson. B* **112**, 275 (1996).
249. H. Ponstingl and G. Otting, *J. Biomol. NMR* **9**, 441 (1997).
250. T. Parella, F. Sánchez-Ferrando and A. Virgili, *J. Magn. Reson. A* **112**, 106 (1995).
251. T. Parella, F. Sánchez-Ferrando and A. Virgili, *J. Magn. Reson. A* **114**, 32 (1995).
252. S. Stelten and D. Leibfritz, *Magn. Reson. Chem.* **33**, 827 (1995).
253. T. Fäcke and S. Berger, *Magn. Reson. Chem.* **33**, 144 (1995).
254. T. Fäcke and S. Berger, *Tetrahedron* **51**, 3521 (1995).
255. T. Fäcke and S. Berger, *J. Magn. Reson. A* **119**, 260 (1996).
256. T. Nishida, G. Widmalm and P. Sandor, *Magn. Reson. Chem.* **34**, 377 (1996).
257. T. Parella, unpublished work.
258. T. Fäcke and S. Berger, *J. Am. Chem. Soc.* **117**, 9547 (1995).
259. C. Roumestand, J. Mispelter, C. Austruy and D. Canet, *J. Magn. Reson. B* **109**, 153 (1995).
260. J. M. Bernassau and J. M. Nuzillard, *J. Magn. Reson. A* **108**, 248 (1994).
261. M. Guéron and P. Plateau, in *Encyclopedia of NMR*, edited by R. K. Harris and D. M. Grant, Vol. 8, p. 4931. Wiley, Chichester (1996).
262. C. Dhalluin, J.-M. Wieruszeski and G. Lippens, *J. Magn. Reson. B* **111**, 168 (1996).
263. D. B. Fulton, R. Hrabal and F. Ni, *J. Biomol. NMR* **8**, 213 (1996).
264. G. Lippens, C. Dhalluin and J.-M. Wieruszeski, *J. Biomol. NMR* **5**, 327 (1995).
265. S. J. F. Vincent, C. Zwahlen and G. Bodenhausen, *J. Biomol. NMR* **7**, 169 (1996).
266. S. J. F. Vincent, C. Zwhalen, P. H. Bolton, T. M. Logan and G. Bodenhausen, *J. Am. Chem. Soc.* **118**, 3531 (1996).
267. (a) D. B. Fulton and F. Ni, *J. Magn. Reson.* **129**, 93 (1997); (b) M. Mescher, A. Tannus, M. O. Johnson and M. Garwood, *J. Magn. Reson. A* **123**, 226 (1996).
268. A. Haase, J. Frahm, W. Haenicke and D. Matthei, *Phys. Med. Biol.* **30**, 341 (1985).
269. R. J. Ogg, P. B. Kingsley and J. S. Taylor, *J. Magn. Reson. B* **104**, 1 (1994).
270. W. S. Price and Y. Arata, *J. Magn. Reson. B* **112**, 190 (1996).
271. W. S. Price, K. Hayamizu and Y. Arata, *J. Magn. Reson.* **126**, 256 (1997).
272. P. C. M. van Zijl and C. T. W. Moonen, *J. Magn. Reson.* **87**, 18 (1990).
273. E. O. Stejskal and J. E. Tanner, *J. Chem. Phys.* **42**, 288 (1965).
274. K. F. Morris and C. S. Johnson, Jr, *J. Am. Chem. Soc.* **114**, 3139 (1992).
275. K. F. Morris and C. S. Johnson, Jr, *J. Am. Chem. Soc.* **115**, 4291 (1993).
276. K. F. Morris, C. S. Johnson, Jr and T. C. Wong, *J. Phys. Chem.* **98**, 603 (1993).
277. K. F. Morris, P. Stilbs and C. S. Johnson, Jr, *Anal. Chem.* **66**, 211 (1994).
278. A. Jerschow and N. Muller, *J. Magn. Reson.* **125**, 372 (1997).
279. H. Barjat, G. A. Morris, S. Smart, A. G. Swanson and S. C. R. Williams, *J. Magn. Reson. B* **108**, 170 (1995).
280. E. K. Gozansky and D. G. Gorenstein, *J. Magn. Reson. B* **111**, 94 (1996).
281. D. Wu, A. Chen and C. S. Johnson, Jr, *J. Magn. Reson. A* **121**, 88 (1996).
282. N. Birlirakis and E. Guittet, *J. Am. Chem. Soc.* **118**, 13083 (1996).
283. A. Jerschow and N. Muller, *J. Magn. Reson. A* **123**, 222 (1996).
284. M. Lin and M. J. Shapiro, *J. Org. Chem.* **61**, 7617 (1996).
285. M. Lin, M. J. Shapiro and J. R. Wareing, *J. Am. Chem. Soc.* **119**, 5249 (1997).
286. C. Dalvit and J. M. Böhlen, *NMR Biomed.* in press.
287. D. Wu, A. Chen and C. S. Johnson, Jr, *J. Magn. Reson. A* **123**, 215 (1996).
288. C. S. Johnson, Jr, *J. Magn. Reson. A* **102**, 214 (1993).
289. A. Chen, D. Wu and C. S. Johnson, Jr, *J. Am. Chem. Soc.* **117**, 7965 (1995).
290. A. S. Altieri, D. P. Hinton and R. A. Byrd, *J. Am. Chem. Soc.* **117**, 7566 (1995).
291. A. J. Dingley, J. P. MacKay, G. L. Shaw, B. D. Hambly and G. F. King, *J. Biomol. NMR* **10**, 1 (1997).
292. A. J. Dingley, J. P. MacKay, M. B. Morris, B. E. Chapman, P. W. Kuchel, B. D. Hambly and G. F. King, *J. Biomol. NMR* **6**, 321 (1995).
293. E. Ilyina, V. Roongta, H. Pan, C. Woodward and K. H. Mayo,

Biochemistry **36**, 3383 (1997).

294. J. Lapham, J. P. Rife, P. B. Moore and D. M. Crothers, *J. Biomol. NMR* **10**, 255 (1997).

295. J. A. Jones, D. K. Wilkins, L. J. Smith and C. M. Dobson, *J. Biomol. NMR* **10**, 199 (1997).

296. A. Gafni and Y. Cohen, *J. Org. Chem.* **62**, 120 (1997).

297. O. Mayzel and Y. Cohen, *J. Chem. Soc., Chem. Commun.* 1901 (1994).

298. O. Mayzel, O. Aleksiuk, F. Grynszpan, S. E. Biali and Y. Cohen, *J. Chem. Soc., Chem. Commun.* 1183 (1995).

299. O. Mayzel, A. Gafni and Y. Cohen, *J. Chem. Soc., Chem. Commun.* 916 (1996).

300. K. F. Morris and C. S. Johnson, Jr, *J. Am. Chem. Soc.* **114**, 776 (1992).

301. K. F. Morris and C. S. Johnson, Jr, *J. Magn. Reson. A* **101**, 67 (1993).

302. M. Liu, J. K. Nicholson and J. C. Lindon, *Anal. Chem.* **68**, 3370 (1996).

303. P. Mutzenhardt and D. Canet, *J. Chem. Phys.* **105**, 4405 (1996).

304. R. Dupeyre, P. Devoulon, D. Bourgeois and M. Décorps, *J. Magn. Reson.* **95**, 589 (1991).

305. E. Mischler, F. Humbert, B. Diter and D. Canet, *J. Magn. Reson. B* **106**, 32 (1995).

306. D. Canet, *Prog. Nucl. Magn. Reson. Spectrosc.* **30**, 101 (1997).

307. D. Canet, in *Encyclopedia of NMR*, edited by R. K. Harris and D. M. Grant, Vol. 6, p. 3938. Wiley, Chichester (1996).

308. D. Canet and M. Décorps, in *Dynamics of Solutions and Fluids Mixtures by NMR*, edited by J.-J. Delpuech, p. 310. Wiley, Chichester (1995).

309. D. Canet, J. Brondeau, E. Mischler and F. Humbert, *J. Magn. Reson. A* **105**, 239 (1993).

310. D. G. Cory and W. E. Maas, *J. Magn. Reson. A* **106**, 256 (1994).

311. W. E. Maas, F. Laukien and D. G. Cory, *J. Magn. Reson. A* **103**, 115 (1993).

312. P. Mutzenhardt, J. Brondeau and D. Canet, *J. Magn. Reson. A* **108**, 110 (1994).

313. C. D. Eads, *J. Magn. Reson. A* **107**, 109 (1994).

314. J. Brondeau, P. Mutzenhardt, J. M. Tyburn and D. Canet, *J. Magn. Reson. B* **109**, 310 (1995).

315. D. G. Cory, F. Laukien and W. E. Maas, *J. Magn. Reson. A* **105**, 223 (1993).

316. J. Brondeau, D. Boudot, P. Mutzenhardt and D. Canet, *J. Magn. Reson.* **100**, 611 (1992).

317. W. E. Maas and D. G. Cory, *J. Magn. Reson. A* **114**, 229 (1995).

318. P. Mutzenhardt, J. Brondeau and D. Canet, *J. Magn. Reson. A* **117**, 278 (1995).

319. A. Sodickson and D. G. Cory, *J. Magn. Reson.* **125**, 340 (1997).